Preferred Latitudes of the Intertropical Convergence Zone

DUANE E. WALISER* AND RICHARD C. J. SOMERVILLE

Climate Research Division, Scripps Institution of Oceanography, University of California, San Diego, La Jolla, California

(Manuscript received 8 January 1993, in final form 25 October 1993)

ABSTRACT

The latitude preference of the intertropical convergence zone (ITCZ) is examined on the basis of observations, theory, and a modeling analysis. Observations show that convection is enhanced at latitudes of about 4° to 10° relative to the equator, even in regions where the sea surface temperature (SST) is maximum on the equator. Both linear shallow-water theory and a moist primitive equation model suggest a new explanation for the off-equatorial latitude preference of the ITCZ that requires neither the existence of zonally propagating disturbances nor an off-equatorial maximum in SST. The shallow-water theory indicates that a finite-width, zonally oriented, midtropospheric heat source (i.e., an ITCZ) produces the greatest local low-level convergence when placed a finite distance away from the equator. This result suggests that an ITCZ is most likely to be supported via low-level convergence of moist energy when located at these "preferred" latitudes away from the equator. For a plausible range of heating widths and damping parameters, the theoretically predicted latitude is approximately equal to the observed position(s) of the ITCZ(s). Analysis with an axially symmetric, moist, primitive equation model indicates that when the latent heating field is allowed to be determined internally, a positive feedback develops between the midtropospheric latent heating and the low-level convergence, with the effect of enhancing the organization of convection at latitudes of about 4° to 12°. Numerical experiments show that 1) two peaks in convective precipitation develop straddling the equator when the SST maximum is located on the equator; 2) steady ITCZ-like structures form only when the SST maximum is located away from the equator; and 3) peaks in convection can develop away from the maximum in SST, with a particular preference for latitudes of about 4° to 12°, even in the ("cold") hemisphere without the SST maximum. The relationship between this mechanism and earlier theories is discussed, as are implications for the coupled ocean–atmosphere system and the roles played by midlevel latent heating and SST gradients in forcing the low-level atmospheric circulation in the tropics.

1. Introduction

The intertropical convergence zone (ITCZ) is one of the most prominent and important features of the tropical atmosphere. This region of enhanced cloudiness and rainfall constitutes the upward branch of the Hadley circulation, and, in a general sense, marks the earth's meteorological equator. The conversion of latent and sensible to potential energy in the convecting systems of the ITCZ acts to stabilize the tropical troposphere, which is heated from the ocean below, and plays an important role in the atmospheric energy cycle, particularly in the transport of heat to the extratropics. Furthermore, the extensive cloudiness associated with the ITCZ contributes significantly to the planetary albedo, and thus to the planetary energy balance. While it is clear that the ITCZ plays a fundamental and important role in the earth's climate, there are still elementary questions pertaining to the ITCZ that remain unresolved.

Figure 1 displays the long-term (1975–87) mean structure of the ITCZ using highly reflective cloud data (HRC; Garcia 1985). This dataset uses subjectively analyzed daily visible and infrared satellite mosaics to measure the frequency of occurrence of large-scale organized convective systems. The monthly dataset is composed of "images" with a 1° spatial resolution, where the values denote the number of days in a given month that the "pixels" were covered by deep, organized tropical convective systems. The HRC dataset has been shown by Waliser et al. (1993) to compare qualitatively well with other indices of tropical convection [i.e., outgoing longwave radiation (OLR) and International Satellite Cloud Climatology Project (ISCCP) Stage C2 convective index], and has been applied by Waliser and Gautier (1993) in the development of a global climatology of the ITCZ. The HRC map illustrates three fundamental characteristics of the time-averaged ITCZ whose explanation remains incomplete. First, the convection associated with the ITCZ is suppressed over the equator at nearly all oceanic longitudes, even in regions with no corresponding minima in SST. Second, the bulk of the convection is generally

Corresponding author address: Prof. Duane E. Waliser, State University of New York, Endeavour Hall 129, Institute for Terrestrial and Planetary Atmospheres, Stony Brook, Stony Brook, NY 11794-5000.

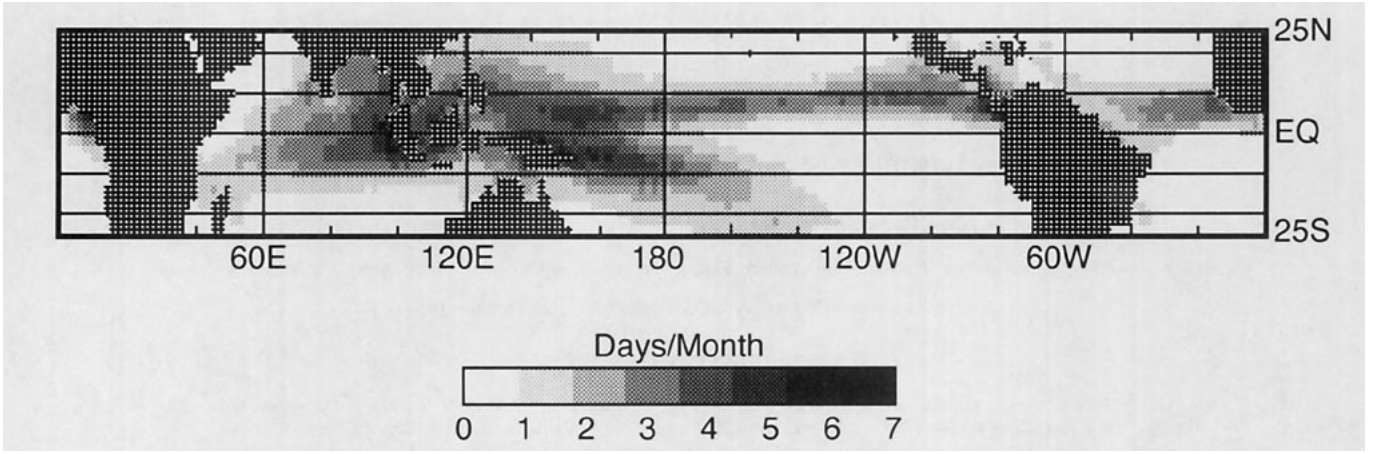

FIG. 1. Long-term mean HRC (1975–87).

located between about 4° and 12° from the equator. Third, this off-equatorial enhancement of convection generally favors the Northern Hemisphere.

The goal of this study is to investigate the reasons behind the first two of the above characteristics, that is, why the ITCZ, in general, is located away from the equator, and at about 4° to 12° latitude. Such an understanding is a useful, if not necessary, starting point for the understanding of the third characteristic—the preference of the ITCZ to reside in the Northern Hemisphere. While there has been an extensive amount of research on a wide variety of topics concerning the ITCZ,[1] investigations directly addressing the latitude position of the ITCZ have been rare, and theories for its explanation even more so. In the following section, a brief review of previous theories pertaining to the latitude preference of the ITCZ(s), along with important related studies, will be presented. In section 3, steady-state, linear, shallow-water theory will be developed and used to reveal the dependence of the low-level convergence field on the latitude of an idealized ITCZ. In section 4, an axially symmetric moist primitive equation atmospheric model will be employed in an analogous manner to examine the relationship between precipitation maxima (ITCZs) and the latitude of the (imposed) SST maximum. In section 5, a discussion of the results and their implications will be given.

2. Review of previous studies and theories

Early observational studies, such as that of Bjerknes et al. (1969), indicated that the spatial distribution of SST, particularly the presence of equatorial upwelling, plays an important role in displacing the ITCZ away from the equator. Figure 2 shows the long-term mean monthly SST (Reynolds 1988) constructed from the same time period as the HRC field shown in Fig. 1. Inspection of Figs. 1 and 2 shows that the spatial structures of the HRC and SST are indeed highly correlated, with the ITCZ being nearly coincident with the warm ($\geq$27°C) water regions of the tropics. These two figures, along with the many studies relating warm surface water to enhanced deep convection (e.g., Ichiye and Petersen 1963; Graham and Barnett 1987), offer some support for the idea that SST forcing is largely responsible for the spatial structure of tropical deep convection, and thus the spatial structure of the ITCZ(s). The importance of this forcing mechanism as it relates to the preferred latitudes of the ITCZ was most firmly established by Pike (1971), who employed an axially symmetric, coupled ocean–atmosphere model to study ITCZ formation. Pike found that in his model, the ITCZ developed over the SST maximum, which for his coupled system was located away from the equator due to induced equatorial ocean upwelling.

A second explanation for off-equatorial ITCZs was given by Charney (1971), who analyzed ITCZ formation for an atmosphere whose organization of convection was governed by conditional instability of the second kind (CISK). CISK is the growth of an instability in a moist, conditionally unstable atmosphere that is caused by the positive feedback between the upper-level latent heat release and the frictional convergence in the boundary layer. The upper-level heating modifies the large-scale flow, increasing the frictional convergence of moisture in the boundary layer, which feeds the upper-level heat source (Charney and Eliassen 1964). From the results of his analysis, Charney hypothesized that for a zonally symmetric CISK system, the position of the ITCZ is governed by a balance between two processes: 1) the Ekman pumping efficiency of moist energy out of the atmospheric boundary layer, which increases with the Coriolis parameter (and thus

[1] An in-depth review of the earliest studies concerning the Hadley circulation is given in Lorenz (1967). Brief reviews of more recent ITCZ dynamics literature can be found in Goswami et al. (1983), Lindzen (1990), Hess et al. (1992), and Waliser (1992).

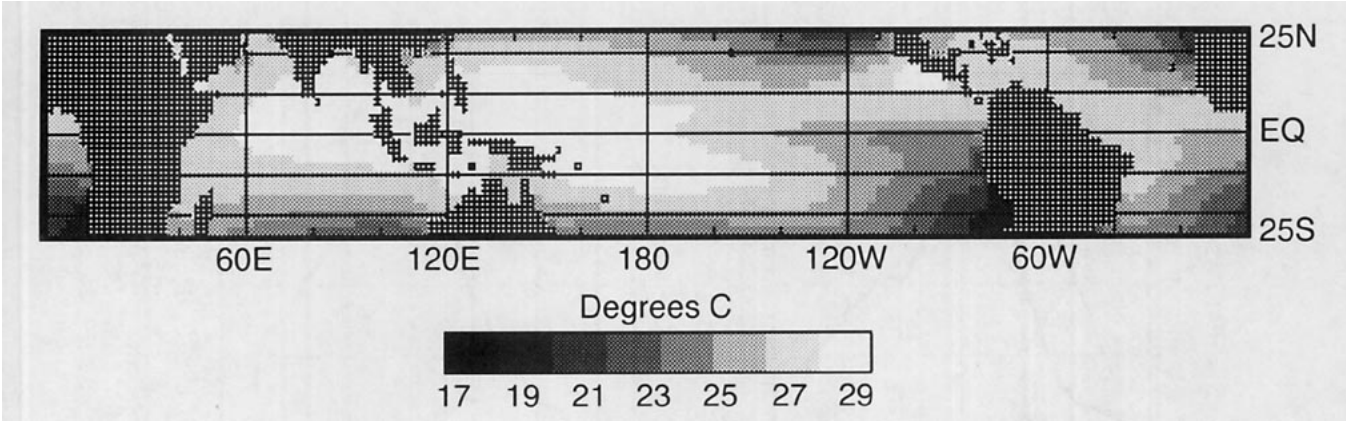

FIG. 2. Long-term mean SST (1975–87).

latitude), and 2) the boundary-layer supply of moist energy, which, in general, decreases with latitude. At some optimal latitude away from the equator, these two processes in combination will determine the most likely position for the ITCZ to develop.

A third explanation resulted from Holton et al.'s (1971) analysis of a linearized, barotropic model of the tropical boundary layer. Holton et al. showed that the boundary-layer convergence due to a zonally propagating wave tends to be concentrated at a critical latitude where the angular frequency of the disturbance equals the Coriolis frequency. They also note that the often-observed 4–5-day tropical "easterly" waves (Reed and Recker 1971; Yanai 1968; Salby et al. 1990) would have a critical latitude of about 6°. From these results, Holton et al. and Holton (1974) argue that zonally propagating equatorial disturbances may be responsible for organizing convection at the observed latitudes of the ITCZ, and thus for the latitude placement of the ITCZ itself.

A fourth explanation was offered by Lindzen (1974) from the results of an analysis of wave–CISK. In this case, the low-level tropical convergence field results from inviscid internal wave fields rather than Ekman pumping. The analysis indicated the existence of 1) a wave–CISK mode, independent of longitude, with a period of about 4.8 days, and 2) traveling disturbances arising from longitudinal inhomogeneities in the tropics with similar periods and zonal scales of about 10° to 30°. The oscillatory system resulting from the coupling of these two modes leads to maximum low-level convergence (and thus a maximum in convection) in regions centered at about 6° to 7°.

In considering the four explanations above, it is important to note that the mechanisms associated with the studies of Pike (i.e., ocean upwelling) and Charney can be manifested in an axially symmetric framework, and those of Charney, Holton et al., and Lindzen can be manifested even when the SST maximum is located at the equator. These considerations motivate two important questions.

First, is the presence of equatorial ocean upwelling—that is, SST maxima away from the equator—required for the formation of an off-equatorial ITCZ? Figure 3 shows coincident profiles of SST and HRC as a function of latitude for four tropical ocean domains. These data indicate that while the SST distribution does appear to have a strong influence on the convection profile, particularly in regions of strong equatorial upwelling, the meridional distribution of SST is not likely to account for the moderate double peak in convection in the warm-pool regions. This latter point suggests that a dynamical mechanism in the atmosphere is acting to enhance convection at these off-equatorial latitudes. Indeed, three-dimensional general circulation modeling (GCM) studies, such as those by Hayashi and Sumi (1986) and Hess et al. (1992), show that double ITCZs form (at about 7°N and 7°S) even when the SST maximum is on the equator. These observations and modeling results suggest that the answer to this first question is no, that is, SST maxima away from the equator are not required for the formation of off-equatorial, or double, ITCZs.

Second, in the case when SST is maximum on the equator, are zonally propagating disturbances required for an off-equatorial ITCZ to form, or can an axially symmetric system (such as Charney's) support an ITCZ away from the equator? Few studies have addressed this question. Schneider and Lindzen (1977) performed a test of Charney's hypothesis using an axially symmetric, linearized, primitive equation model. Their results suggested that the most likely position for the ITCZ to develop would be on the equator, rather than away from the equator as suggested by Charney. Moreover, the GCM study by Hess et al. (1992) showed evidence that zonally propagating equatorial waves may indeed be responsible for the formation of off-equatorial, or double, ITCZs. In their study, the double ITCZ that formed straddling the equator in a three-dimensional "aqua-planet" simulation, with the SST maximum on the equator, collapsed into a single ITCZ at the equator when the integration was continued

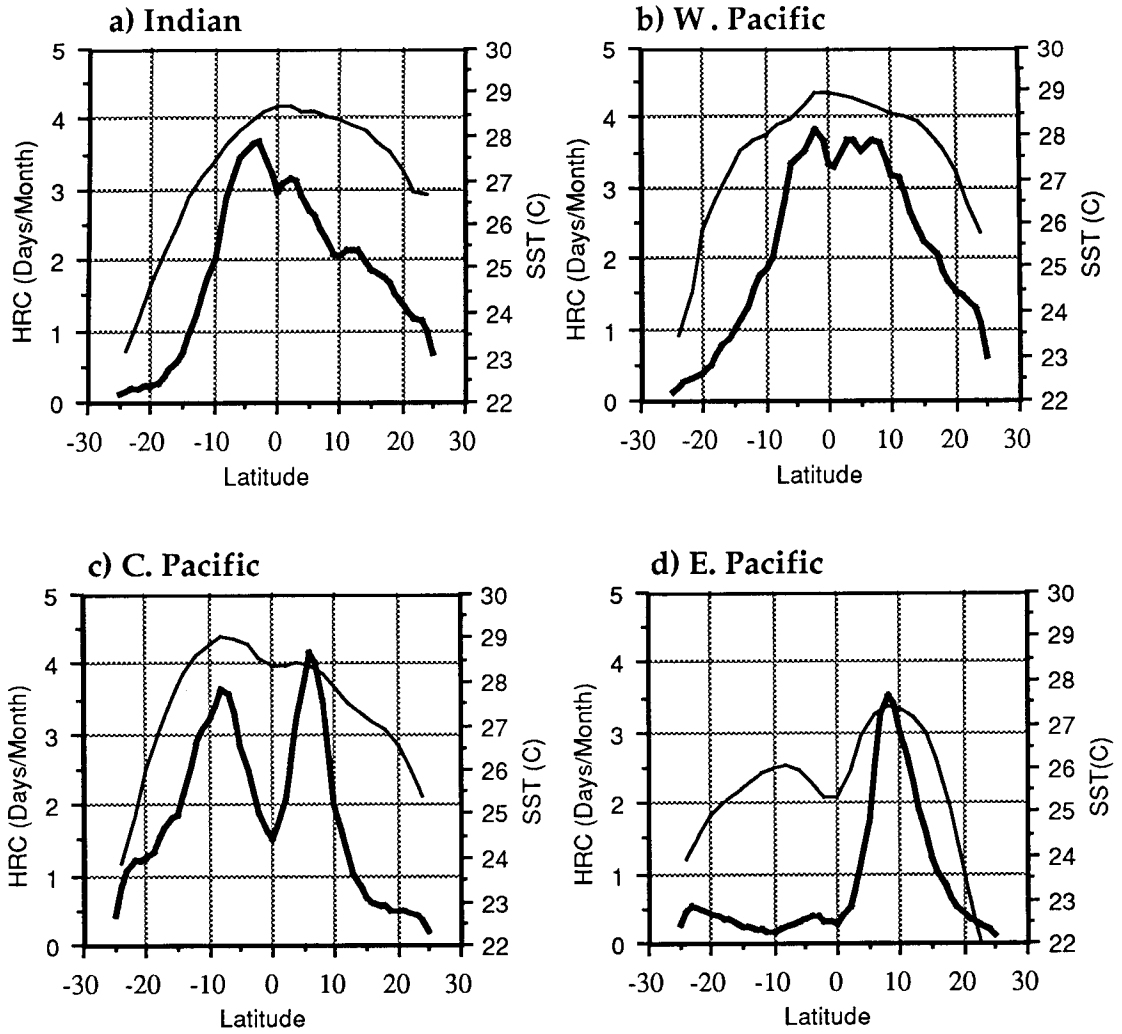

FIG. 3. Long-term (1971–87) mean meridional profiles of HRC (thick) and SST (thin) for the regions denoted: (a) 60°–80°E, (b) 110°–150°E, (c) 160°E–160°W, and (d) 100°–140°W. HRC and SST data have 1° and 2° grid resolution, respectively.

under the constraint of zonal symmetry. Hess et al. attributed this feature to convection-organizing equatorial waves, most readily identified as mixed Rossby–gravity waves. Both the above studies suggest that an axially symmetric system cannot support an off-equatorial ITCZ when the SST maximum is on the equator. In fact, the results from Hess et al. tend to support the Holton et al. hypothesis that the spatial structure of the preferred wave modes in the tropics may be setting the latitude scale for the formation of the ITCZ.

The objective of this study is to further examine the latitude preference of the ITCZ. Our results, which are in contrast to those just described, suggest that zonally propagating disturbances may not be required for the development of off-equatorial ITCZs, even when the SST maximum is on the equator. Furthermore, they provide an additional explanation for the observed off-equatorial latitude preference for the ITCZ. In the next two sections, a two-step approach, simple theory followed by numerical modeling, is undertaken in order to reveal the fundamental dynamics underlying the off-equatorial latitude preference of the ITCZ. For additional details, see Waliser (1992).

3. Analysis using simple linear theory

a. Theoretical framework and background

In this section, linear, steady-state, shallow-water theory is developed and employed to study the dependence of the low-level convergence on the latitude of imposed zonally oriented heat sources (i.e., ITCZs). The theoretical framework is based on Matsuno (1966). The equations in nondimensional form are

$$\epsilon u - \frac{1}{2} yv = -\frac{\partial p}{\partial x} \tag{3.1}$$

$$\epsilon v + \frac{1}{2} yu = -\frac{\partial p}{\partial y} \tag{3.2}$$

$$\alpha p + \frac{\partial u}{\partial x} + \frac{\partial v}{\partial y} = -Q, \tag{3.3}$$

where y and x are distances northward (from the equator) and eastward, u and v are the zonal and meridional velocities, p is the pressure perturbation, Q is the heat source, and ϵ and α are the mechanical and thermal damping rates, respectively. For positive heating ($Q > 0$), the values of u and v correspond to the lower layer, and p corresponds to the perturbation at the surface. The heat source Q increases the amount of high potential energy fluid in the system, and thus in some sense is a representation of a midtropospheric heat source (e.g., moist deep convection).

Gill (1980) used this theoretical model to study tropical circulations produced by idealistic imposed heat sources and found that it qualitatively recreated principal aspects of the tropical atmospheric circulation (e.g., Walker and Hadley circulations, monsoon flows). Zebiak (1982, 1986) extended the above model to simulate surface wind anomalies in the equatorial Pacific during El Niño by parameterizing Q in terms of SST anomalies and by adding a convergence feedback mechanism. Other applications of simplified shallow-water theoretical models to the tropical atmosphere include Webster (1972), Philander et al. (1984), and Hirst (1986).

In the solutions presented below, the equivalent depth is specified to be 325 m. This gives a length scale $[(c/2\beta)^{1/2} = R_0]$ of about 1100 km ($\sim 10°$) and a time scale $[(2\beta c)^{-1/2}]$ of about 0.23 days. However, the results emphasized in this section hold for a wide range of equivalent depths. The equations (3.1)–(3.3) are solved numerically by reducing the problem to a second-order differential equation in v and then solving by the method described by Zebiak (1982).

It is important to point out that given a proper transformation of the depth scales and damping times, the model specified above has been shown by Neelin (1989) to be analogous in form to the boundary-layer model of Lindzen and Nigam (1987). As posed, the simple model (3.1)–(3.3) presumes a two-layer troposphere with the forcing represented as midtropospheric heating in the height equation. The Lindzen and Nigam scheme models the tropical boundary layer with the forcing represented by SST gradients in the momentum equations. These SST gradients are communicated to the atmospheric boundary layer by turbulent exchange from the surface, giving rise to low-level density gradients, and thus to low-level pressure gradients. These pressure gradients force the low-level tropical wind field and thus help determine the distribution of deep convection. The formal equivalence of these two models implies that the "behavior" discussed below is qualitatively the same for either formulation (i.e., whether peak $Q(x, y)$ represents a maximum in midtropospheric heating or SST); however, the interpretation of how these results apply to the formation of the ITCZ differs. The contrast in these two formulations and their implications on the nature of the results will be addressed further in sections 4 and 5.

b. Zonally symmetric results

In this section the zonally symmetric form of (3.1)–(3.3) is employed to study the dependence of the low-level atmospheric response on the meridional position of a zonally symmetric heat source. Gill (1980) solved these equations (ignoring the ϵv term) for the case of a delta-function heat source placed at $y = 1.0$ to simulate the wind field produced by ITCZ-like heating. In addition, Gill showed that for the case of a meridionally broad heat source, off-equatorial heating leads to large asymmetries in the model "Hadley cells," with the "winter" ("summer") cell becoming significantly stronger (weaker). Using modifications to the Hadley circulation theory of Held and Hou (1980), and numerical simulations, Lindzen and Hou (1988) showed in considerably more detail the degree to which winter cell mass fluxes increase and summer cell mass fluxes decrease, when peak atmospheric heating is moved even slightly away from the equator. Lindzen and Hou used these results to explain why the annually averaged Hadley circulation is much larger than the circulation forced by the annually averaged heating. In a similar study, Hack et al. (1989) showed that the winter cell mass flux was greatest when the imposed maximum in atmospheric diabatic heating (i.e., the ITCZ) was placed at about 10°. Hou and Lindzen (1992) went on to show how the strength of the Hadley circulation is also sensitive to the width of the imposed, internal tropical heat source. In the above studies, the ITCZ was a passive, specified entity, and the circulation was studied for a given prescribed latitude of the "ITCZ." The intention here is to examine the dependence of the low-level convergence on the position of the heating maximum and interpret the results in terms of the strength and stability of the heat source itself (i.e., the ITCZ).

Figure 4 shows one solution of the model equations for heating centered away from the equator ($y_0 = 1.0$). The figure shows low-level u and v, dv/dy, and Q (represented as a Gaussian with e-folding scale 0.7). The model produces a low-level convergence and negative pressure perturbation (not shown) in the region of the heating maximum, two easterly jets, and one westerly jet on the equatorial side of the heating maximum. Of interest here is how the low-level convergence field, specifically the value associated with the maximum heating, depends on the meridional position of the imposed heat source. The low-level convergence is es-

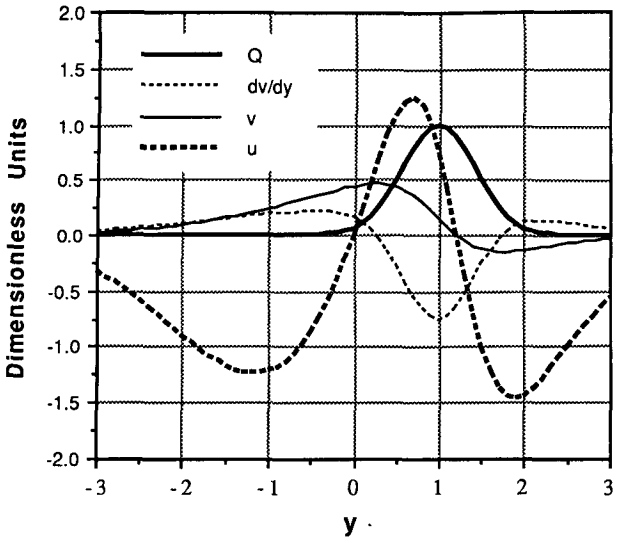

FIG. 4. Solution to zonally symmetric, linear, shallow-water model with Gaussian heating profile (e-folding 0.7) centered on $y = 1.0$. Damping parameters are $\epsilon = \alpha = 0.1$ (2.3 days^{-1}).

pecially important since the midtropospheric heat sources in the tropics (e.g., moist deep convection) are predominantly fueled by low-level convergence of heat and moisture. Figure 5 shows the low-layer convergence values coincident with the location of maximum heating as a function of heat source width and "latitude." The figure shows that the greatest amount of low-level convergence occurs when the heat source is placed a finite distance away from the equator. The distance away from the equator is greater for larger heating widths. Furthermore, the plot shows that as the heat source becomes narrow, the solution asymptotes to the delta-function heating solution found by Gill; in that case, there is no dependence of the local low-level convergence on the position of the heating maximum. The results shown in Fig. 5 are qualitatively the same as those obtained when the equations are solved using spherical geometry, or when a range of equivalent depths, thought applicable to the tropical atmosphere (40–600 m; Gill 1982), is applied.

Further exploration of the model parameter space shows that the qualitative nature of the above result, that is, low-level convergence at the latitude of the heat source is maximum when the heating is a finite distance away from the equator, is nearly independent of the values of α and ϵ. Figure 6 shows the dependence of the low-level convergence as a function of heating position for α and ϵ differing by up to two orders of magnitude. Only in the case of high mechanical damping (e-folding time about 1/4 day) is the convergence maximum greatest for equatorial heating. The sensitivities displayed in Figs. 5 and 6 of the model convergence field to the width of the heating and the magnitude of the mechanical damping are intimately related to the ITCZ/CISK-related conclusions of Schneider and Lindzen (1977), who found, contrary to Charney's hypothesis, that the most unstable CISK perturbation occurred on the equator. Although their model was based on a set of linearized primitive equations, their experimental setup was very similar to that discussed here, and a comparison of the two analyses highlights parameterization dependencies that may be related to their final conclusion.

Schneider and Lindzen (1977) investigated (see their Fig. 10) the strength of the vertical velocity at the top of the boundary layer as a function of the latitude of an imposed heat source in order to determine the latitude preference for frictional convergence in the boundary layer due to upper-level heating (CISK). The heat source used in their experiment had an e-folding width of about 1.5° and corresponds roughly to the smallest heating width shown in Fig. 5. Their model eddy viscosity coefficient in the boundary layer was 50 m^2 s^{-1}, decreased to 1 m^2 s^{-1} at the top of the boundary layer, and remained at this value in the free atmosphere. They found that the greatest vertical velocity occurred when the imposed heat source was located on the equator and diminished as the heat source was moved poleward. This behavior is very similar to that exhibited by the shallow-water model analyzed here when applying either a narrow heating width or a high mechanical damping rate (Figs. 5 and 6; note $w = -\partial v/\partial y$). Thus, the conclusion of Schneider and

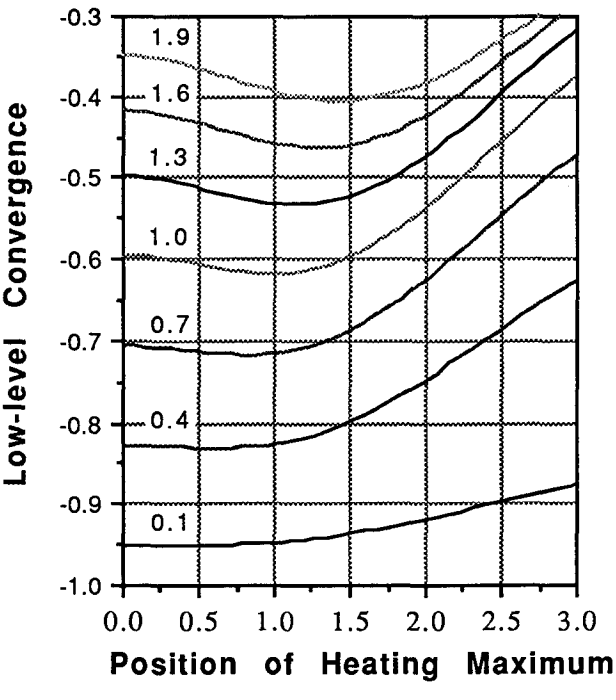

FIG. 5. Low-level convergence (dv/dy) at heating maximum as a function of the meridional position of the heating maximum. Results are plotted for a range of heating profile widths (given in Gaussian e-folding distance). Damping rates are as in Fig. 4.

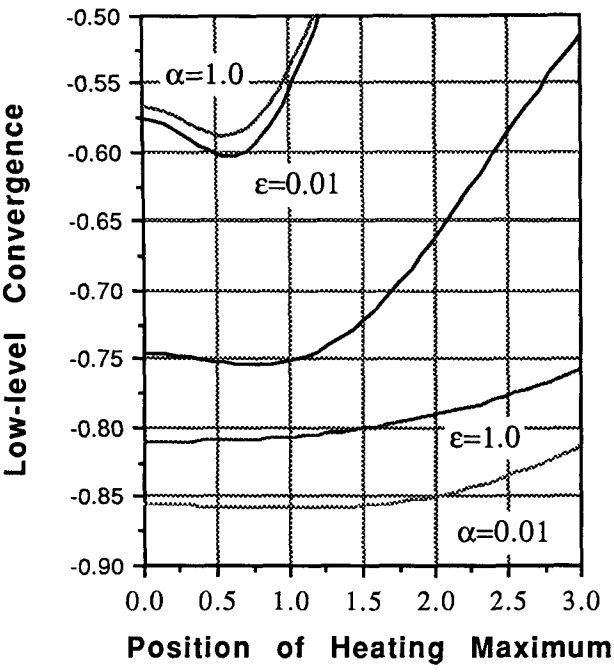

FIG. 6. Low-level convergence (dv/dy) at heating maximum as a function of the meridional position of the heating maximum. Results are plotted for a range of damping rates. Unless otherwise noted, $\epsilon = \alpha = 0.1$ (2.3 day^{-1}). Heating profile width is 0.7.

Lindzen is likely to be dependent on the width of the imposed heat source and magnitude of the internal eddy viscosity, with the indication that, in their study, a slightly wider heat source width or lower viscosity would have produced the greatest "CISK perturbation" slightly away from the equator, and actually provided support for Charney's hypothesis.

The dependence of the low-level convergence on the "latitude" of the imposed heat source can be understood by considering the low-level momentum balance. When the (finite width) heat source is on the equator, the meridional pressure gradients to the north and south are each balanced by some combination of friction and geostrophy. When the heat source is displaced slightly away from the equator, the pressure gradient equatorward of the heat source becomes predominantly balanced by friction, while the pressure gradient poleward of the heat source becomes primarily balanced by geostrophy. These changes in the momentum balance result in a rapid growth of the meridional velocity on the equatorward side of the heat source (depending on the value of ϵ) and modest decline of the meridional velocity on the poleward side of the heat source. Thus, the low-level convergence, which in the zonally symmetric case is determined by the difference between these two opposing meridional velocities, increases. As the heat source is moved far from the equator, both equatorward and poleward pressure gradients become primarily balanced by geostrophy, the meridional velocities diminish, and the low-level convergence decreases. In an analysis of tropical boundary-layer flows, Young (1988) develops the notion of a transitional latitude between midlatitude and near-equatorial flow that is proportional to the ratio of surface drag and rotation (i.e., $y = \kappa/\beta$), and thus in the present system, this latitude would be roughly proportional to ϵ.

Together, the above results illustrate that for a finite-width, line-oriented heat source (e.g., ITCZ), and reasonable choices of heating widths and damping parameters, the maximum low-level convergence is obtained when the heat source is displaced away from the equator at a distance of about one equatorial Rossby radius (4° to 12°). As mentioned earlier, the relationship between the low-level convergence and the position of the heat source is an important one, since tropical diabatic heat sources are largely supported by low-level convergence of heat and moisture. Thus, while it is important to show that there is a particular latitude range where (imposed) midlevel heating will induce the greatest low-level convergence, it is also important to note that this range of latitude is also where the low-level convergence will most likely be able to support, or fuel, the imposed diabatic heat source. Further, such a relationship between heating and induced convergence might well lead to a positive feedback that would enhance the strength of the heat source. These questions will be considered in more detail in section 4 through the use of a moist, primitive equation model and will be discussed further in section 5.

Of additional importance to the notion of an equilibrium position of the ITCZ is the dependence of the total energy of the system and the overall mass flux on the latitude of the heat source. Figure 7 shows the total energy (kinetic plus potential) and total mass flux plotted in a manner analogous to Figs. 5 and 6. The solutions shown in this figure use the same model parameters as those in Fig. 4. Also plotted in the figure are the vertical velocity ($w = -\partial v/\partial y$) over the heat source maxima. Each of the parameters are in dimensionless units and have been normalized by their values for heating centered on the equator. The figure shows that, in addition to producing the greatest low-level convergence (i.e., midlevel vertical velocity), the solution with off-equatorial heating produces the greatest mass overturning (e.g., Lindzen and Hou 1989; Hack et al. 1989) and lowest total energy.

c. *Zonally asymmetric results*

The results using the zonally symmetric model shed important light on the questions of the latitude dependence of the strength and stability of the ITCZ and the associated atmospheric energy states. However, the zonally symmetric equations have the unfortunate feature that the zonal wind is always zero on the equator (Fig. 4). This produces some unrealistic features in the model wind fields, as has been noted by Lindzen and Nigam

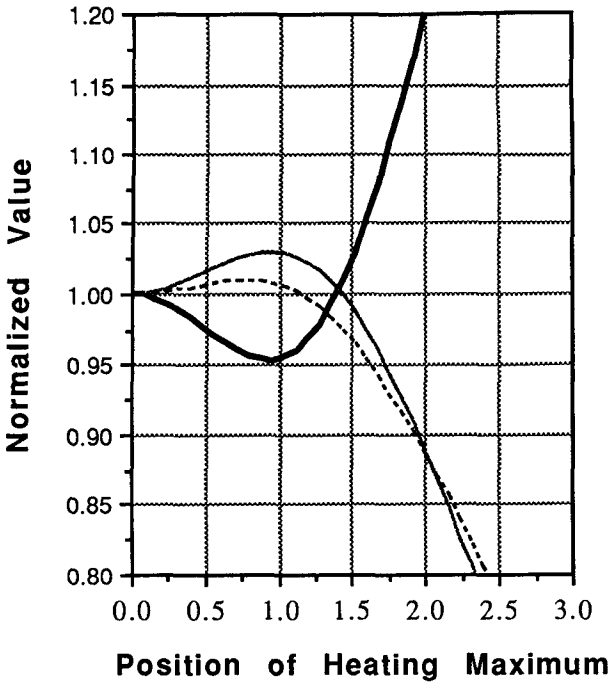

FIG. 7. Total energy, mass overturning, and vertical velocity ($dv/dy = -w$) as a function of the meridional position of the heat source. Heating width and damping parameters are chosen as in Fig. 4. Values are plotted in dimensionless units, normalized by their value for equatorial heating.

(1987) and Neelin (1988). The purpose of this section is to analyze briefly the model behavior for zonally asymmetric heating in a manner analogous to that in the previous subsection to ensure that the conclusions based on the results above are not unique to the zonally symmetric formulation. For this more general framework, a wavenumber one modulation is added to the zonally symmetric ITCZ-like heat source. Solutions to the full equations (3.1)–(3.3) are computed as a function of heat source latitude, with some exploration of the model parameters.

Figure 8 shows the model solution for a base case using the full equations. This solution was found for the ITCZ-like heat source placed at $y = 1.0$ and a zonal wavenumber one modulation of amplitude 0.5. This forcing field is a very crude estimate of the observed ITCZ field shown in Fig. 1. The remaining model parameters are the same as those for the solution shown in Fig. 4. Shown is the heating field (Q), divergence field ($\partial u/\partial x + \partial v/\partial y$), pressure perturbation (p), and wind field (u and v). The solution is similar to those shown by Gill (1980) and Zebiak (1982) for similar forcing functions. Figure 9a is a two-dimensional analog to Figs. 5 and 6. At each longitude, the value of the convergence overlying the heat source is given as a function of the heat source "latitude." The line superimposed on the figure is the meridional position where the heating field produced the maximum low-level convergence. For example, west of about 60°E the convergence was maximum when the heat source was on the equator, and at about 90°W, the convergence maximum occurred when the heat source was located at about $y = 1.5$. Figures 9b through 9f are the same as Fig. 9a with the exception that in each case one model parameter has been modified from its base case value. The results from the zonally asymmetric model shown in the previous two figures demonstrate that the near-equatorial behavior exhibited by the zonally symmetric model is not an artifact of zonally symmetry. The low-level convergence is greatest over most, if not all, "longitudes" when the heating is displaced away from the equator. Further, the model total energy exhibits a similar dependence on heat source latitude, and is lowest when the heat source is located at about $y_0 = 1.0$ (for the parameters chosen).

4. Analysis using axially symmetric primitive equation model

The results from the steady-state, linear, shallow-water theory analyzed in the previous section suggest that an "ITCZ" is likely to be best supported, in terms of induced low-level convergence, when placed away from the equator. The advantages of the shallow-water model are its simplicity in terms of specification and interpretation. The disadvantages, however, are that it requires prescribing the internal atmospheric heat source and then analyzes the resulting circulation. In reality, the heat source and the circulation are intimately coupled. Additionally, the model is linear and encompasses no feedbacks, such as nonlinearities in the dynamics or due to latent heat release. For this reason, we next analyze the problem in an analogous manner with an axially symmetric, moist, primitive equation model. Axially symmetric models have been employed and found to be particularly instructive in a number of ITCZ (e.g., Pike 1971; Bates 1970; Goswami et al. 1983; Charney et al. 1988) and climate-related (e.g., MacCracken 1988) studies. The experiments presented here are designed to determine if the behavior exhibited by the simple, linear model is manifested when moist, nonlinear dynamics are taken into account. The most important distinguishing feature of these experiments compared to those of the previous section is that the internal atmospheric heat source (i.e., the ITCZ) is not specified but is allowed to form in an internally and physically consistent manner. A similar approach was taken by Davey and Gill (1987) who incorporated a latent heat feedback into the Gill (1982) model to examine its effects on idealized simulations of the atmospheric circulation in the tropics.

a. Model description

The numerical model is an axially symmetric, moist, primitive equation model with a pole-to-pole domain and ocean-only surface conditions. The model employs

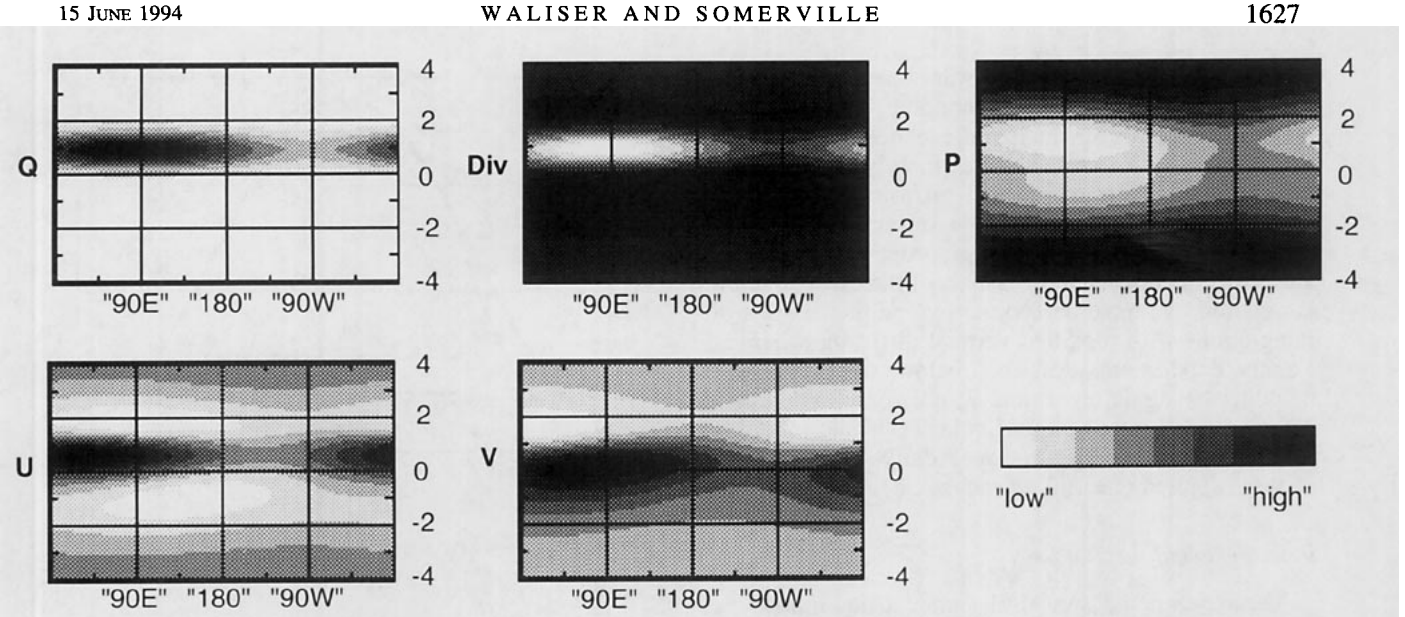

FIG. 8. Solution to full model equations (3.1)–(3.3) for zonally asymmetric line-oriented heat source placed at $y = 1.0$. Fields shown are Q, low-level divergence, pressure perturbation, and wind field (u, v). All values are dimensionless and scaled to the same range. Heating width and damping parameters are the same as those for Fig. 4. Wavenumber one modulation of the heat source has a amplitude of 0.5.

the B-grid numerical method of Arakawa and Lamb (1977) with the improved vertical differencing scheme developed by Arakawa and Suarez (1983). The model equations and constants are given in appendix A. Condensation processes are modeled using the moist-convective scheme of Emanuel (1991) and a simple large-scale condensation parameterization (Williamson et al. 1987). Explicit shortwave and longwave radiation calculations are included using the scheme of Morcrette (1990). Bulk aerodynamic surface fluxes are computed from a specified, fixed sea surface temperature. Vertical and horizontal diffusion are modeled as large-scale

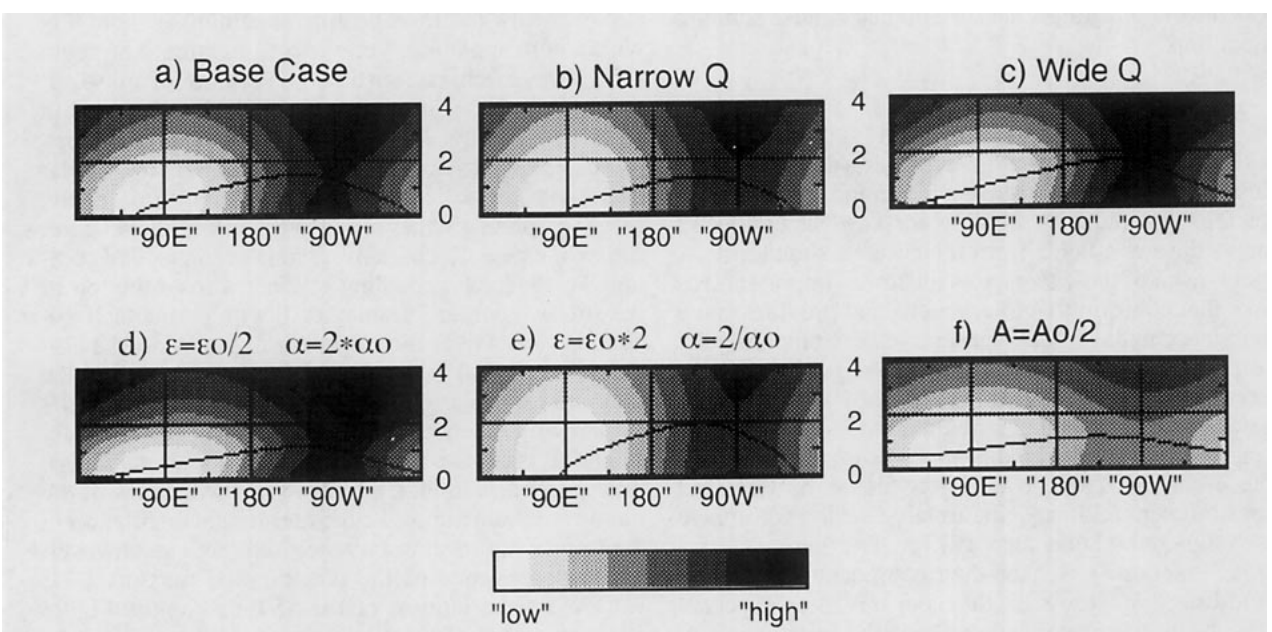

FIG. 9. Low-level convergence at heating maximum (with respect to latitude) as a function of the meridional position of the heat source. A two-dimensional analog to Figs. 5 and 6. (a) Base case; parameters are those for the solution shown in Fig. 8. (b) Meridional heat source width equal to 0.4. (c) Meridional heat source width equal to 1.0. (d) Mechanical damping 0.05 and thermal damping 2.0. (e) Mechanical damping 2.0 and thermal damping 0.05. (f) Amplitude of wavenumber one zonal modulation set to 0.25. Lines imposed on figures denote for each "longitude" the meridional position of the heat source that produced the maximum low-level convergence.

eddy diffusive fluxes with constant coefficients. Since our principal objective is to elaborate on the shallow-water experiments in which midlevel heating forces the atmospheric flow, we have intentionally chosen a relatively small value of vertical diffusion through the planetary boundary layer so that surface forcing does not mask this effect. However, in order to test the sensitivity of the results to this aspect of the model parameterization, we have performed two additional sets of integrations with modified vertical diffusion schemes. For the experiments described below, the model grid contains 19 sigma levels and 2° horizontal resolution. Interactions between cloud liquid water and radiation are ignored and a time-averaged daily solar radiation cycle is applied (i.e., no diurnal cycle).

b. *Experimental setup*

The experimental setup is designed to determine how the the strength and character of the ITCZ depends on the latitude of the SST maximum. Five simulations were performed, each differing only in the latitude of the SST maximum, which changes from 0° to 16° in 4° increments. These experiments are denoted case 0, 4, 8, 12, and 16. The SST profile for case 0 is taken to be a sine-squared approximation to the observed zonally averaged profile. Figure 10 shows the idealized SST profile and the observed zonally averaged SST profile computed from the SST dataset mentioned earlier. The idealized SST profile was shifted northward at 4° increments for cases 4–16. Each simulation was integrated from a resting state for 300 days under equinox conditions.

c. *Results*

Figure 11 shows the time-averaged (day 200–300) zonal wind, mass streamfunction, moist-convective heating, and radiative cooling for case 0. Figure 12 shows the same fields from the case 12 simulation. A comparison of these two cases illustrates important features that conform to earlier results and provides some confidence in the model's performance. Comparing the case 0 zonal winds to zonally averaged, equinoctial observations (Oort 1983) shows that they have approximately the right spatial distribution but a slightly higher magnitude (~20%) in the upper-level westerly jets. These enhanced upper-level jets are to be expected since momentum fluxes due to large-scale eddies have been ignored (Schneider 1977). The case 0 mass streamfunction is weaker than equinoctial conditions would suggest. However, this is also is to be expected when heating is centered directly on the equator (Lindzen and Hou 1988). The character of the north–south asymmetries for the case 12 zonal wind fields (Fig. 12a) and tropical region mass streamfunctions (Fig. 12b) are reasonably consistent with observations (Oort and Rasmusson 1970; Oort 1983) and previous studies

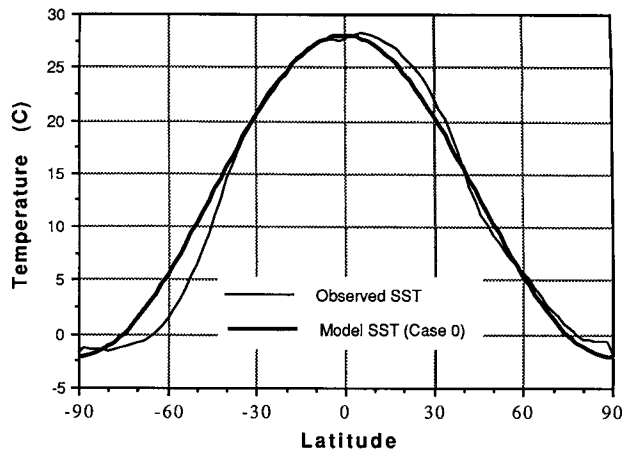

FIG. 10. Long-term (1972–1987) zonally averaged monthly SST (thin) and sine-squared approximation used in primitive equation model (case 0; thick).

such as those by Lindzen and Hou (1988) and Hess et al. (1992). The magnitude of the "winter" cell mass streamfunction for case 12 (a case with an SST profile resembling solstitial conditions) exhibits values similar to the observed zonally averaged mass flux in solstitial conditions (Oort 1983).

The convective heating rates between the two cases (Figs. 11c and 12c) exhibit profound differences in the tropical region. In case 0, tropospheric latent heating is broad and relatively weak, while case 12 exhibits a strong narrow midlevel heating maximum at about 8°N with a corresponding, yet weaker, maximum at about 4°S. This last characteristic is the feature of most importance in these simulations and will be discussed in more detail below. The radiative heating fields (shortwave plus longwave) illustrate characteristics similar to the convective heating fields. In the midtroposphere, case 0 exhibits a rather broad and weak midlevel cooling, while case 12 contains regions of intensified cooling. This enhanced cooling originates from the top of the strong "winter" Hadley cell, with particularly enhanced values over the subsiding region. Case 12 also exhibits a broad low-level region of cooling in the northern tropics originating from the top of the model's "trade wind boundary layer."

The figures discussed above give some confidence that the model simulates qualitatively well some of the more essential features of the meridional circulation in the tropics. Of most importance and interest, however, is the dependence of the precipitation maxima (i.e., ITCZs) on the latitude of the SST maximum. Figure 13 shows time–latitude diagrams of the convective precipitation for the 300 days of simulation between latitudes 40°N and 40°S. There are two features of interest indicated by the precipitation history in these five simulations. The first involves the temporal evolution of the precipitation. In the equatorial and near-equa-

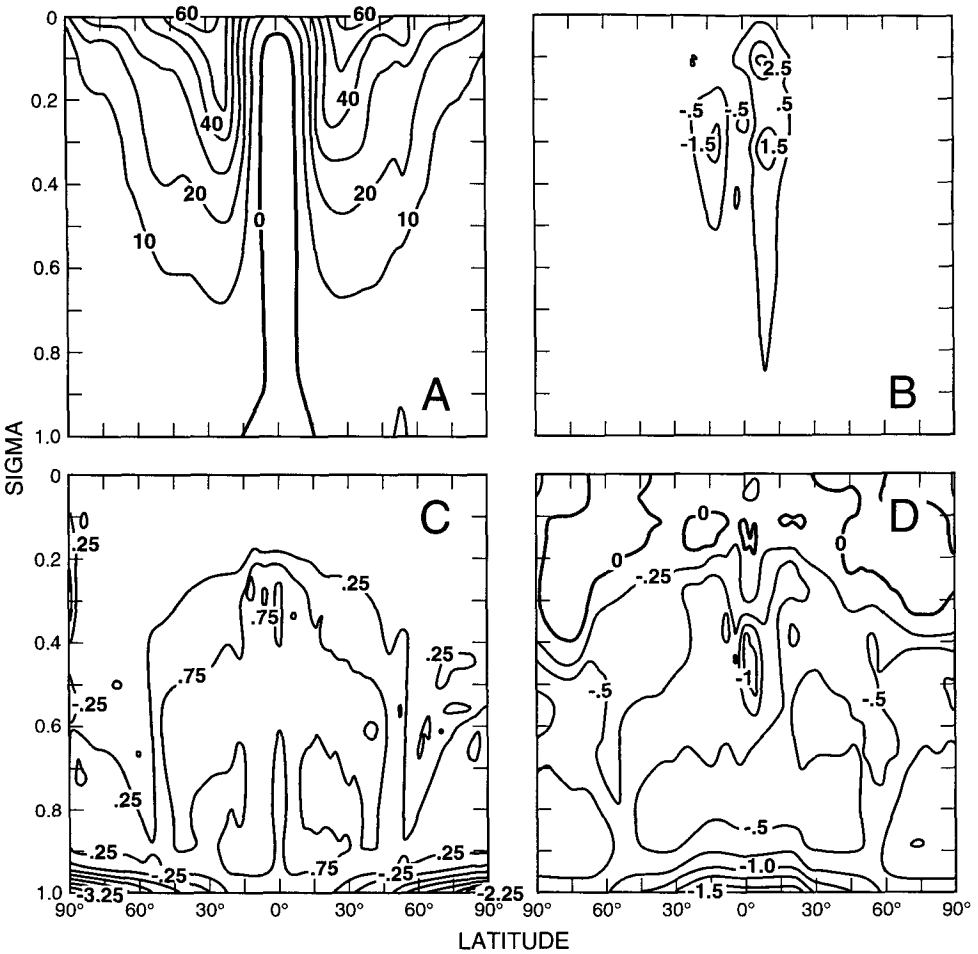

FIG. 11. Case 0 (SST maximum on equator) time-averaged (a) zonal wind, (b) mass streamfunction, (c) convective heating rate, and (d) radiative cooling rate (longwave + shortwave). Time averages are over days 200 to 300. Contour intervals are (a) 10 m s^{-1}, (b) 1.0 × 10^{10} kg s^{-1}, (c) 0.5°C day^{-1}, and (d) 0.25°C day^{-1}. Dashed lines indicate negative values.

torial cases, there is significantly more variability with many transient features throughout the 300-day simulation. Very little indication of a "steady" ITCZ feature is evident, with the heaviest precipitation often associated with the transient activity and occurring over a relatively broad range of latitude (15°N to 15°S). To some extent, cases 4 and 8 begin to show some stable features with precipitation maxima forming on either side of the equator. In the cases where the SST maximum is poleward of 8°N, the model precipitation field exhibits very steady ITCZ-like features.

The second feature illustrated by the time–latitude diagrams is that the precipitation maxima tend to organize in the off-equatorial regions, especially when the SST maximum is displaced away from the equator. This characteristic is better illustrated by comparing the meridional profiles of convective precipitation. Figure 14 shows the time-averaged (day 200–300) convective precipitation for the five simulations. This figure contains two very curious and important features: 1) precipitation minima tend to occur over the equator, and an enhancement of precipitation occurs on both sides of the equator at latitudes of about 4° to 10° regardless of the latitude of the SST maximum; and 2) the precipitation maximum is not always located over the maximum SST but tends to favor latitudes of about 8° (N and S). Also important but not unexpected is the fact that the precipitation maximum on the warm side of the equator is, in general, stronger than the maximum on the cold side.

To test the sensitivity of the above results to the specification of vertical diffusion, we have performed two additional sets of integrations. In the first sensitivity test, the coefficient of vertical diffusion was set to 5 m^2 s^{-1} near the surface, decreasing to the "free atmosphere" value of 0.2 m^2 s^{-1} at about 1.2 km. These simulations started from day 300 of the standard experiments described above and were integrated for 200

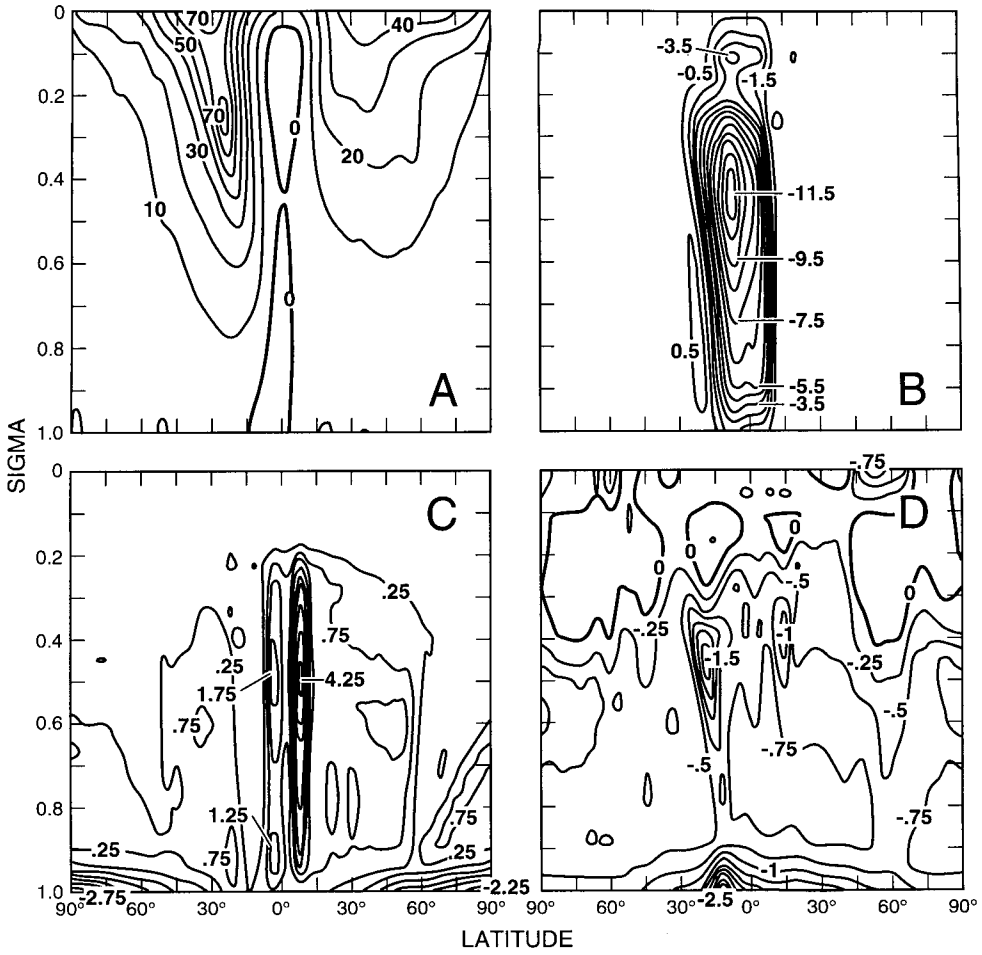

FIG. 12. Same as Fig. 11 except for case 12 (SST maximum at 12°N).

days. The time-averaged precipitation from these simulations is shown in Fig. 15a. In the second test, the constant-coefficient vertical diffusion scheme was replaced by a Richardson number–dependent scheme (Williamson et al. 1987), with a minimum threshold value of K_σ equal to 0.2 $m^2 s^{-1}$. These simulations also started from day 300 of the standard experiments and were integrated for 100 days. Note that, except for mid- and high latitudes, the computed vertical diffusion in this second test largely remained at 0.2 $m^2 s^{-1}$. The time-averaged precipitation from these simulations is shown in Fig. 15b. Inspection of the plots in Fig. 15 shows that the essential character of the numerical results remains the same: in general, there are two peaks in precipitation independent of the latitude of the SST maximum, and these peaks generally occur between 4° and 8°.

The above features are particularly important, since they tend to suggest that 1) an ITCZ constrained to the equatorial and very near-equatorial latitudes is not as "stable" or intense as one that is able to form at some distance away from the equator ($\gtrsim$6°); 2) convection can develop away from the maximum in SST, with a particular preference for latitudes of about 4° to 12°; and 3) consistent with some earlier studies (e.g., Lindzen and Hou 1988; Hack et al. 1989), off-equatorial heating (or SST maxima) lead to stronger meridional circulations and thus in these cases to enhanced precipitation maxima. These results are consistent with the discussion of observations in sections 1 and 2, especially Fig. 3. The particularly interesting feature of the above model result is the fact that the "cold" hemisphere can support a modest peak in precipitation. Examination of observed profiles of SST and HRC demonstrates that a similar feature occurs in some domains of the tropical oceans. Figure 16 shows (a) January–March and (b) July–September long-term mean SST and HRC profiles for the region 130°–170°E. Also shown (Fig. 16c) are the time-averaged precipitation and SST profiles for case 12, a simulation with a similar SST profile. In both the observed and model cases, the "convection" peaks at about 8° in the warm hemi-

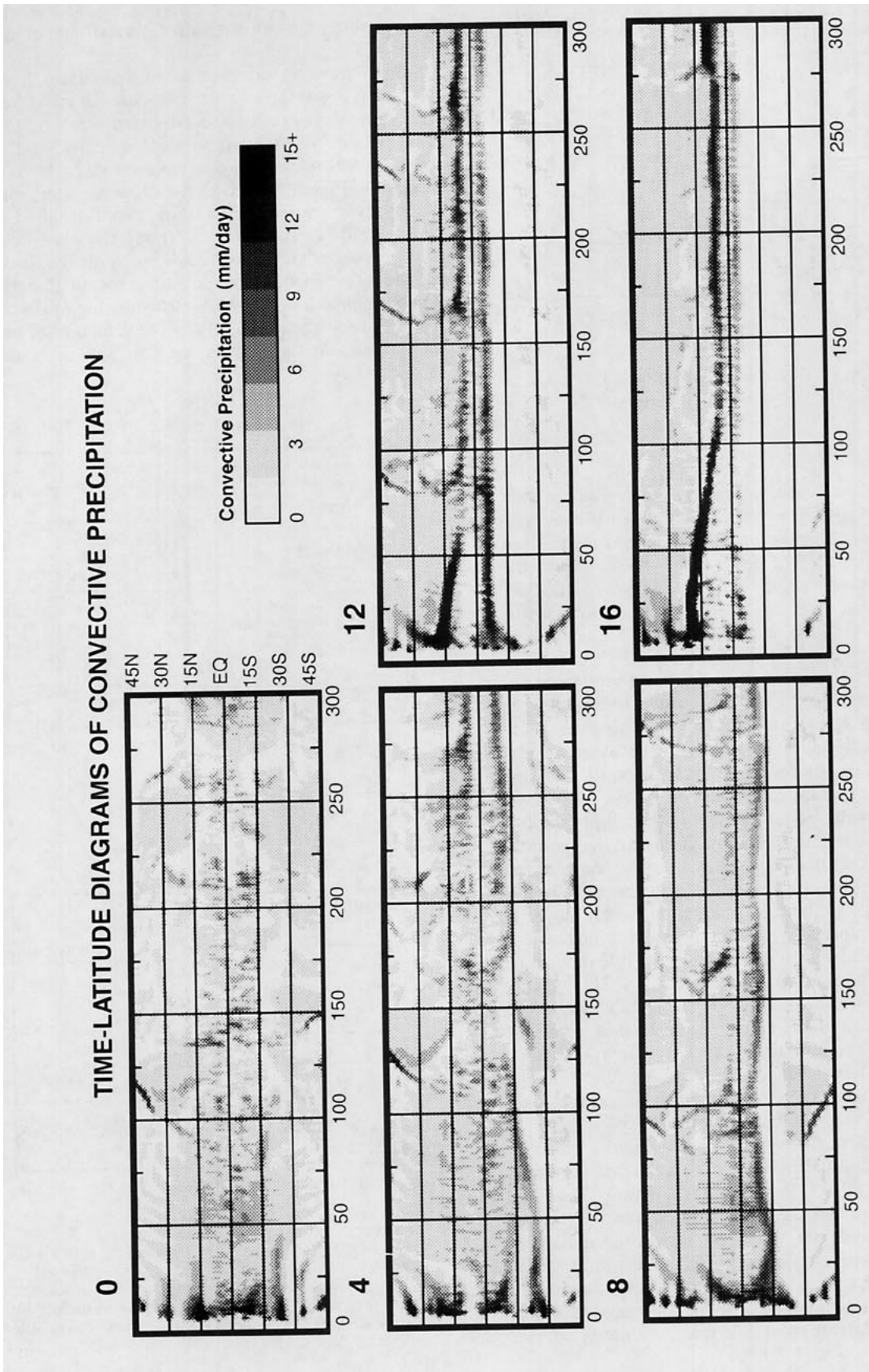

FIG. 13. Time–latitude diagrams of convective precipitation for cases 0–16.

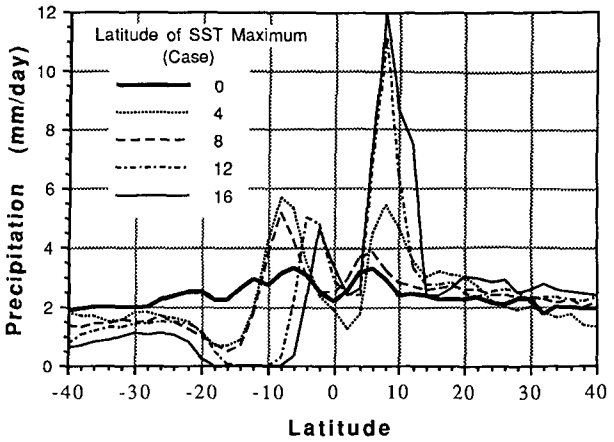

FIG. 14. Time-averaged (day 200–300) convective precipitation profiles.

sphere, near the SST maximum, and a smaller peak exists in the cold hemisphere at about 4°. However, it should be noted that the minor peak in the observations occurs over an SST of about 28°C, while that in the model occurs over an SST of only about 26°C, an SST lower than that often associated with convective formation (e.g., Graham and Barnett 1987).

Together with the theoretical results discussed in section 3, the results from the primitive equation model suggest that the midtropospheric convective heating itself is playing an important role in organizing these off-equatorial precipitation maxima. This behavior has important implications for the interpretation of the simplified theory presented in section 3. As mentioned earlier, the results from this theory could apply to both 1) the Gill model interpretation, implying that midtropospheric heating displaced away from the equator produces the greatest low-level convergence; and 2) the Lindzen–Nigam model interpretation, where an SST maximum displaced away from the equator induces the greatest boundary-layer convergence. While the nature of the observations shown in Figs. 3 and 16 suggests that forcing by meridional SST gradients is not likely responsible for both off-equatorial peaks in convection, it is instructive to investigate this aspect in more detail. In order to help determine the role that midlevel latent heating may be playing in feeding back on the low-level circulation to establish or enhance these zones of stable convection, the case 0–16 simulations were extended an additional 200 days with the condensation processes turned off. In these cases, denoted case 0d, 4d, 8d, 12d, and 16d, the forcing is solely due to surface temperature gradients, interactions with the radiation, and dry convective adjustment (Manabe and Strickler 1964). In each of the experiments, the specific humidity (which mainly interacts with the longwave radiation in these experiments) was held fixed in a configuration symmetric about the equator with the maximum at the equator.

Although there is no precipitation field in these "dry" cases, it is informative to compare the low-level vertical velocities of the two sets of experiments. In the tropics, regions of upward vertical velocity in the boundary layer are nearly synonymous with regions of precipitation. Figure 17 shows the time-averaged vertical velocity averaged over a sigma depth of 0.8–1.0 for (a) cases 0–16 (day 200–300) and (b) cases 0d–16d (day 450–500). As expected, the vertical velocities of the moist simulations are almost identical to the precipitation profiles (Fig. 14), each showing peaks on both sides of the equator. The vertical velocities of the dry simulations are different in one main and important

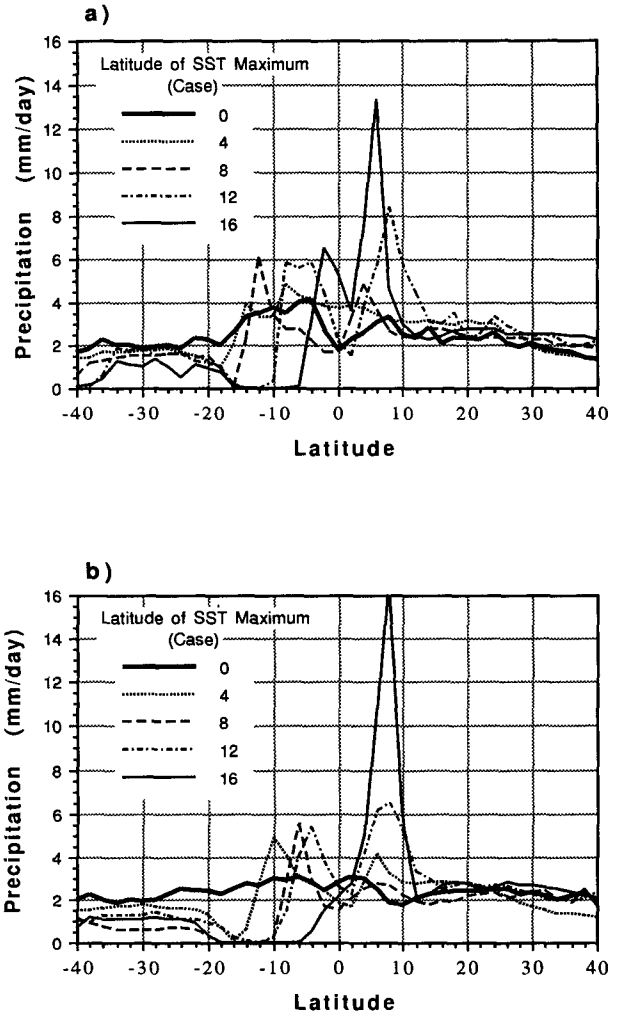

FIG. 15. (a) Time-averaged (day 450–500) convective precipitation profiles for sensitivity simulations in which the coefficient of vertical diffusion was increased to 5 $m^2 s^{-1}$ near the surface. (b) Time-averaged (day 350–400) convective precipitation profiles for sensitivity simulations in which the vertical diffusion scheme was Richardson number dependent. (See section 4c for details.)

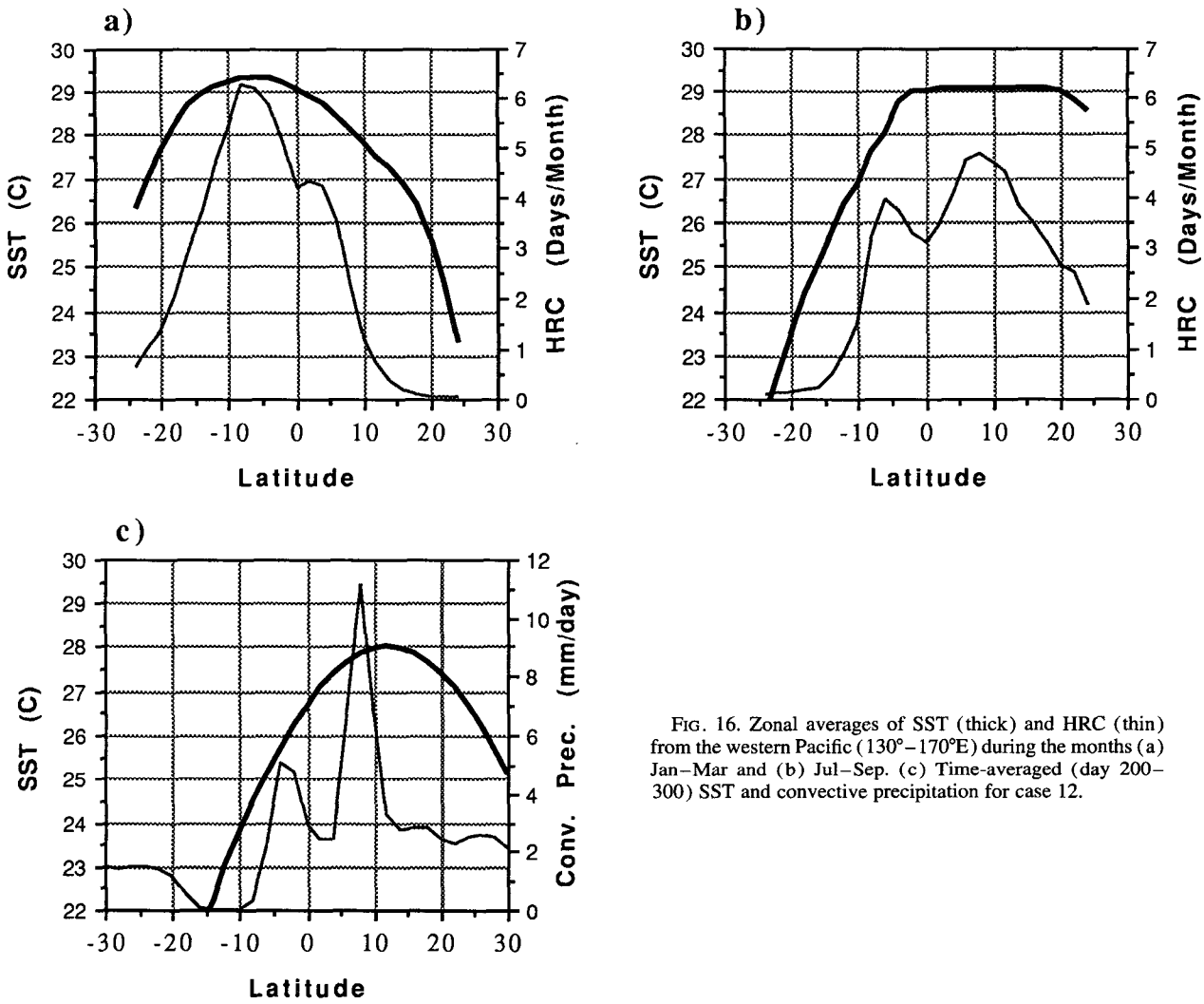

FIG. 16. Zonal averages of SST (thick) and HRC (thin) from the western Pacific (130°–170°E) during the months (a) Jan–Mar and (b) Jul–Sep. (c) Time-averaged (day 200–300) SST and convective precipitation for case 12.

aspect: there are no upward vertical velocity peaks in the Southern (cold) Hemisphere for any of the simulations. Further, the upward velocity peaks in the dry simulations tend to favor the SST maximum more closely than for the moist simulations. This contrast in moist versus dry simulations tends to supports the suggestion that a feedback exists between the midtropospheric latent heating and the low-level convergence of heat and moisture, with the effect of enhancing the zones of convection in the latitude range of about 4°–12°.

5. Discussion and concluding remarks

The objective of this study has been to explain the latitude preference of the ITCZ. Observations of the zonally averaged global ITCZ suggest that the "equilibrium" position is at about 6° to 8°N, with a minor peak in convection at about 6° to 8°S. This off-equatorial latitude preference is often attributed to the spatial distribution of SST, particularly the zones of low SST found along the equator due to equatorial ocean upwelling. The SST and HRC observations shown in Fig. 3 were intended to demonstrate that the spatial distribution of SST, particularly the presence of upwelling, is probably not responsible for the observed enhancements of convection that occur at latitudes of about 4° to 10° (N and S), at least not at all longitudes. From this standpoint, it is clear that dynamical mechanisms within the atmospheric component of the coupled system must be playing a role in enhancing convection at these off-equatorial latitudes, and thus possibly in determining the preferred latitudes of the ITCZ(s).

Results from a simplified, linear theory were particularly important and instructive. These results showed that for a system in which the mechanical damping is not too high (e-folding time $>1/4$ day), a finite-width ITCZ-like heat source displaced a finite distance away

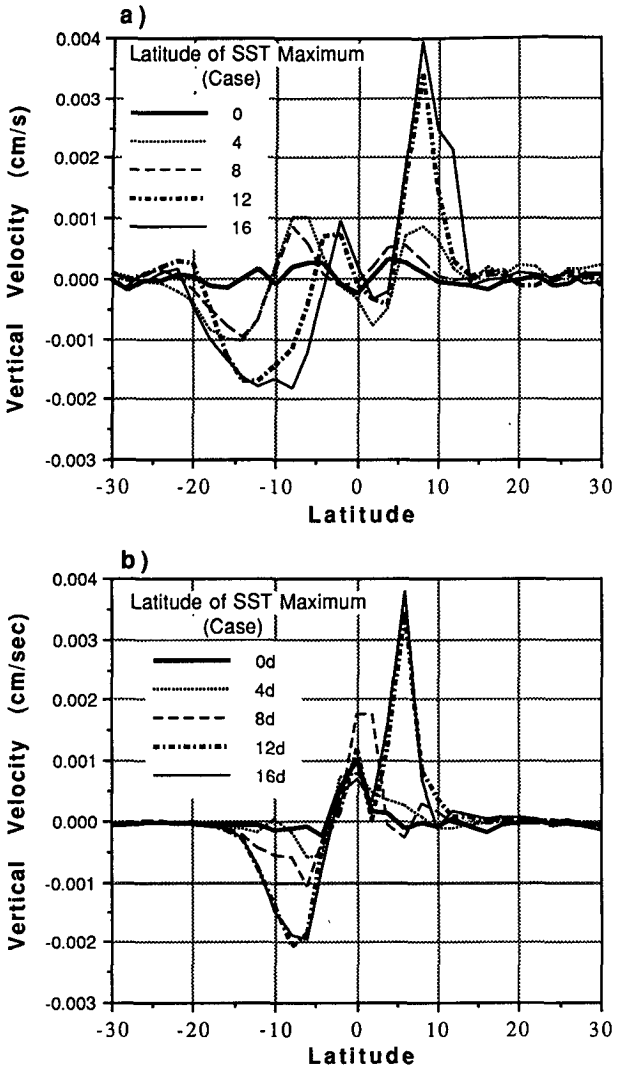

FIG. 17. Boundary-layer depth-averaged (σ = 0.8–1.0) vertical velocity for (a) moist cases 0–16, and (b) dry cases 0d–16d.

from the equator produces the greatest amount of low-level convergence. This behavior results from the requirement that the near-equatorial pressure gradient becomes predominantly balanced by friction as the heat source is moved slightly away from the equator. Such a balance induces the greatest poleward meridional flow and greatest meridional convergence. As the heat source is moved far from the equator, both poleward and equatorward pressure gradients are balanced by geostrophy, which produces very little low-level convergence. This relationship between midlevel heating and induced low-level convergence is important for several reasons. First, tropical atmospheric (latent) heat sources are, to a first approximation, forced and/or supported by low-level convergence of moist energy. Thus, even though these experiments impose the heat source, the results suggest that the heating, which represents moist deep convection, is most likely to be supported via low-level convergence at these "preferred" off-equatorial latitudes. Second, for a plausible range of model parameters, the meridional position of the maximum convergence corresponds very nearly to the latitudes of the observed equilibrium position of the ITCZ. Finally, the results from this simple linear theory suggest that, given a system in which the heat source is not entirely specified but allowed to evolve on its own, it may be possible that a positive feedback could result between the heat source and the low-level convergence field. Such a feedback would lead to "favored" latitudes for the heat sources (ITCZs) to develop and be maintained.

Experiments using a moist, primitive equation model were designed, at least in part, to address if such a feedback would develop. Specifically, the relationship between the model ITCZs and the latitude of the (imposed) SST maximum was examined. The results showed that 1) steady, well-defined ITCZ-like structures formed only when the SST maximum was located away from the equator; and 2) precipitation maxima developed away from the SST maximum, with a particular preference for latitudes of about 4° to 12°, even in the ("cold") hemisphere without the SST maximum. These results indicate that the positive feedback discussed above in the context of the linear theory appears to manifest itself, and that the scales of the model ITCZ heating favor an interaction between the midlevel release of latent heat and the low-level convergence of heat and moisture. In the simulations described here, this interaction is strong enough, for example, to 1) produce a weak double ITCZ when the SST maximum is on the equator, 2) produce a precipitation maximum at about 8°N even when the SST maximum is at 16°N, and 3) produce a small precipitation peak at about 4° to 6° in the hemisphere opposite the SST maximum. Each of these results resembles aspects of the observed meridional profiles of deep convection and SST. The conclusion that midlevel latent heating is playing an important role in the organization of the low-level convergence, and thus producing some of the observed features of the ITCZ, was supported by analogous model runs with internal latent heating turned off (i.e., dry experiments). In contrast to the results of the simulations with latent heating, double peaks in low-level upward vertical velocity did not develop, and the upward vertical motion tended to favor the SST maximum more closely.

The contrast in results between these moist and dry experiments is important when considering the Gill versus Lindzen–Nigam interpretations of the simplified equations (3.1)–(3.3). The convergence forced by an SST maximum, via the Lindzen and Nigam approach, has a dependence on the latitude and width of the SST maximum analogous to that shown in Fig. 5. However, under this interpretation of the equations, a single SST maximum on, or away from, the equator

would not support a double peak in convection, as is indicated by the observations (Fig. 3 and 16) and the results from the moist primitive equation model (Figs. 14–16). Such an interpretation is, however, consistent with the results (and physics) of the dry simulations (cases 0d–16d; Fig. 17). The dependence of the low-level convergence on the position of the heat source (Fig. 5) under the Gill interpretation, however, could support one, or two, ITCZs located at the "preferred" off-equatorial latitudes (i.e., $|y| \sim 1.0$). Once mid-level latent heat sources develop at these preferred latitudes, the associated enhanced strength of the low-level convergence of moist energy would be able to maintain the position and strength of these heat sources.

The above set of results have important implications for the opposing hypotheses of Holton et al. (1971) and Holton (1974) on the one hand, and Charney (1971, 1974) on the other. Holton and collaborators [and in a similar manner, Lindzen (1974)] argued that the spatial structure of the predominant wave modes in the tropics may be setting the scale for the ITCZ, while Charney argued that a preexisting ITCZ determines the dominant wave modes. Observational analysis by Salby et al. (1991) has shown that a significant amount of the convection in the ITCZ regions, particularly at about 8°N and 8°S, is associated with the westward propagation of mixed Rossby–gravity waves (or "easterly waves"). These observations offer some support for Holton's hypothesis, that zonally propagating equatorial waves may determine the position of the ITCZ(s). However, the argument somewhat hinges on the inconsistencies between the results of the axially symmetric experiments presented here and those presented by Hess et al. (1992).

In the experiments by Hess et al., the Community Climate General Circulation Model (CCM1; Williamson et al. 1987) was run in an "aqua-planet" mode with specified SSTs to determine the nature of the ITCZ formation and its effects on the large-scale tropical circulation. Their results showed that for an SST profile with a maximum on the equator (similar to the observed zonal average), a single, intense peak in convection occurred on the equator when a moist-convective adjustment scheme (Manabe et al. 1965) was used for the parameterization of deep convection, and a double peak formed straddling the equator (at about 7°N and 7°S) when a Kuo-type (Kuo 1974) convection scheme was used (cf. Hayashi and Sumi 1986; Sumi 1992). Further, when the Kuo simulation was performed under the constraint of zonal symmetry, the double peak collapsed to a single peak on the equator. This feature was attributed to convection-organizing equatorial waves, most readily identified as mixed Rossby–gravity waves. The results from Hess et al. lend support to Holton's hypothesis that the spatial structure of the preferred wave modes in the tropics may be setting the scale for the formation of the ITCZ.

The results presented in this study suggest that the presence of zonally propagating disturbances (or an off-equatorial SST maximum) are not required for the formation of off-equatorial precipitation maxima, and thus lend support to Charney's (1974) assertion that the off-equatorial latitude preference of the ITCZ may be playing a role in determining the dominant equatorially trapped wave modes. These modes would be those that have a maximum vertical velocity away from the equator, such as the mixed Rossby–gravity wave. However, it should be stressed that while both Charney's hypothesis and the explanation developed here each contain an important feedback between midlevel diabatic heating and low-level convergence, the two theories differ. Charney's theory implies that as the SST maximum moves poleward, the ITCZ should follow and become more stable and intense due to the increase in the Coriolis force. Moreover, the ITCZ should form poleward of the SST maximum where the Coriolis force, and thus the Ekman convergence, is stronger. However, the explanation and results in this study suggest that due to the finite width of the ITCZ, an actual "preferred" latitude range exists, independent, for example, of the SST field. This is best illustrated by Fig. 14, which shows that, as the SST maximum moves poleward, the ITCZ remains at the preferred latitudes, and that a small peak in convection forms at almost a symmetric latitude in the opposite hemisphere.

While the experimental setups of this study and the axially symmetric simulation by Hess et al. are nearly identical, the results are somewhat in conflict. Their axially symmetric case with an equatorial SST maximum yields a single, intense ITCZ peak, while the similar experiment here exhibits two weak precipitation maxima. The reasons for this discrepancy are not clear since a number of relevant model features differ. The gridpoint model used here has 2° resolution and 19 evenly spaced levels, while the spectral model used by Hess et al. uses a 2.8° Gaussian grid with 12 unevenly spaced levels. The lowest two levels in the present model are at 0.947 and 0.895 sigma while in the CCM1 they are at 0.991 and 0.926. The surface flux and diffusion parameterizations in the present model are derived from, and are nearly the same as, those implemented in the CCM1, with the main exception that constant values for eddy diffusivities (except sensitivity test shown in Fig. 15b) and exchange coefficients are applied. These modest differences in model resolution and boundary-layer formulation are possible candidates that may explain the contrasting results. However, it is more likely that the difference in convection schemes may be playing the largest role, specifically their criteria for the onset of convection.

As suggested by the results here, the latent heating field plays an important role in enhancing, and possibly organizing, low-level convergence. It is thus important to point out that the different ways the convection

schemes in the two models release convective available potential energy (CAPE). The Kuo-type scheme releases CAPE only when there is low-level convergence of moisture at the scale of the model grid. This can allow an artificial buildup of CAPE that would otherwise be released by perturbative, small-scale motions in the real atmosphere (Emanuel 1991). The convection scheme implemented in this model is based solely on the one-dimensional moist thermodynamics of each model column. This scheme has the virtue that no artificial dynamical constraints are imposed in determining the onset of convection. Therefore, once convection occurs at what are posed in this paper as "preferred" latitudes, the ensuing feedback due to enhanced low-level convergence at these latitudes maintains the supply of moist energy. In the Kuo-type scheme, the low-level flow in the preferred latitude regions away from an SST maximum may not meet the criteria for convergence and thus never convect, even though the column may be unstable with respect to moist convection. Thus, the feedback discussed here could not be established. These remarks are only to suggest a potential reason for the differences in the outcomes of the two experiments, and should be taken as an acknowledgement of the sensitivity to convective parameterizations, not as evidence for a "best" scheme.

To resolve these issues more decisively, and in particular to explore the sensitivity of these results to several aspects of the parameterizations, it would be helpful to carry out numerical experiments with several modern general circulation models. Ideally, such experiments should be undertaken with models having the capability of switching between competing parameterizations, so that a suite of numerical integrations can be generated differing only in the choice of parameterization, thus facilitating unambiguous intercomparisons.

Finally, we note a possibly significant point of consistency between our results and those of Hess et al. In case 0, that is, SST maximum on the equator, the two off-equatorial precipitation maxima are rather weak (<4 mm day^{-1}; Fig. 14). Therefore, if the mechanism posed above is responsible for this (weak) double "ITCZ," and if such a mechanism influences the selection of the observed equatorial, zonally propagating waves (i.e., Charney's assertion), then the results of Hess et al. could be taken to indicate that these (selected) waves may have a further, and very important, impact on the intensity of the ITCZ(s) when allowed to form in three-dimensional, zonally symmetric, or zonally asymmetric simulations. See Sumi (1992) for an investigation of three-dimensional convective pattern formation in zonally symmetric simulations.

The results from the moist experiments also have relevance to studies of the Hadley circulation, such as those by Schneider and Lindzen (1977), Held and Hou (1980), and Lindzen and Hou (1989). In these studies of the zonal mean meridional circulation, nearly the entire nature of the heat sources is specified. The surface temperature is fixed, and the latent and radiative heating/cooling are combined in the form of a Newtonian relaxation to a radiative–convective equilibrium temperature structure. These conditions allow for minimal feedbacks between the resulting flow and the heat sources. The moist experiments in this study examined the nature of one aspect of these feedbacks—how the strength and character of the tropical convective heat source itself (i.e., ITCZ) depend on the latitude of the SST maximum, with the result that these feedbacks, in addition to the surface temperature distribution, can and may be important in determining the positions of the diabatic heat sources in the tropics. Furthermore, the results indicate that the analyses by Lindzen and Hou (1989), Hack et al. (1989), and Hou and Lindzen (1992), in which the Hadley circulation was analyzed for heating centered away from the equator, may be more applicable to the observed large-scale meridional circulation.

Finally, a conjecture concerning the implications of the above results in terms of the coupled ocean–atmosphere system is warranted. We have noted evidence that appears to indicate the SST field is playing a significant role in determining the location of the ITCZ (Figs. 1–3). However, the theoretical and modeling results presented here show that the off-equatorial latitude preference of the ITCZ may well originate from mechanisms associated with moist atmospheric dynamics; for example, a double ITCZ is possible even when the SST maximum is on the equator. If the constraint of an imposed SST is relaxed, the coupled system itself may evolve to make the off-equatorial ITCZ even more stable. Surface zonal winds from cases 0–16 (not shown) show a strong easterly jet just south of the equator, with mild easterlies on the equator (~ 0.5 m s^{-1}). These easterlies in the near-equatorial region may, depending on the depth of the upper-ocean isothermal layer, result in equatorial surface cooling due to upwelling (e.g., Pike 1971; Charney et al. 1988). This modification to the equatorial circulation could result in more pronounced SST maxima away from the equator. In this coupled configuration, the ITCZ would be considerably more stable due to the additional off-equatorial, low-level convergence driven by the meridional gradients in SST. This (speculative) scenario indicates how the off-equatorial preference of the ITCZ, which appears to originate from atmospheric dynamics, could actually play a role in determining the surface current structure of the tropical oceans, particularly in regions conducive to shallow upper-ocean isothermal layers, such as the eastern Pacific and Atlantic. In these regions, moderate easterlies can produce marked SST maxima away from the equator via equatorial upwelling, and therefore make the ITCZ, which according to our results should initially form at about 4° to 10° away from the equator, even more stable at these off-equatorial latitudes.

Acknowledgments. We thank Catherine Gautier for helping to initiate this study and for moral (and more tangible) support. We thank Nick Graham and Rick Salmon for many insightful discussions and John Roads and Shyh-Chin Chen for help with the numerical model development. We thank Kerry Emanuel for the use of his moist-convection scheme and for sharing his ideas and opinions, Richard Lindzen and David Battisti for offering valuable comments and suggestions, and Jean-Jacques Morcrette for the use of his radiation scheme. Further, we would like to thank two anonymous reviewers and the editor, Peter R. Bannon, for their suggestions, which helped to make the manuscript and numerical experiments more complete.

Much of the funding for this research was provided by the NASA Graduate Student Research Fellowship Program under Grant NGT-50304 and the California Space Institute under Grants CS-88-89 and CS-45-90. Additional support was provided by NASA under Grants NAGW-1978 and NAG5-236. Most of the calculations were done on the Cray Y-MP at the San Diego Supercomputer Center (SDSC) through allocations obtained from SDSC and from the Scripps Institution of Oceanography Block Grant. SDSC was established with, and is principally supported by, grants from the National Science Foundation. A portion of the visualization and illustration utilized software developed by the National Center for Supercomputing Applications at the University of Illinois at Urbana–Champaign. This paper is based on a Ph.D. dissertation (Waliser 1992).

APPENDIX A

Model Formulation

The primitive equation model is formulated as follows:

$$\frac{\partial u}{\partial t} = -\frac{v}{a}\frac{\partial u}{\partial \lambda} - \dot{\sigma}\frac{\partial u}{\partial \sigma} + \left(f + \frac{u\tan\lambda}{a}\right)v + \frac{g}{\Pi}\frac{\partial \tau_u}{\partial \sigma} + \frac{K_H}{a^2\cos\lambda}\frac{\partial}{\partial \lambda}\left(\cos\lambda\frac{\partial u}{\partial \lambda}\right) \quad (4.1)$$

$$\frac{\partial v}{\partial t} = -\frac{v}{a}\frac{\partial v}{\partial \lambda} - \dot{\sigma}\frac{\partial v}{\partial \sigma} - \left(f + \frac{u\tan\lambda}{a}\right)u + \frac{g}{\Pi}\frac{\partial \tau_v}{\partial \sigma} + \frac{K_H}{a^2\cos\lambda}\frac{\partial}{\partial \lambda}\left(\cos\lambda\frac{\partial v}{\partial \lambda}\right) + \frac{1}{a}\frac{\partial \Phi}{\partial \lambda} + \frac{\alpha\sigma}{a}\frac{\partial \Pi}{\partial \lambda} \quad (4.2)$$

$$\frac{\partial \Pi}{\partial t} + \frac{1}{a\cos\lambda}\frac{\partial}{\partial \lambda}(\Pi v\cos\lambda) + \dot{\sigma}\frac{\partial(\Pi\dot{\sigma})}{\partial \sigma} = 0 \quad (4.3)$$

$$\frac{\partial \Phi}{\partial \sigma} = -\alpha\Pi \quad (4.4)$$

$$\frac{\partial \theta}{\partial t} = -\frac{v}{a}\frac{\partial \theta}{\partial \lambda} - \dot{\sigma}\frac{\partial \theta}{\partial \sigma} + \frac{g}{\Pi}\frac{\partial \tau_\theta}{\partial \sigma} + \frac{K_H}{a^2\cos\lambda}\frac{\partial}{\partial \lambda}\left(\cos\lambda\frac{\partial \theta}{\partial \lambda}\right) + Q_R + Q_L \quad (4.5)$$

$$\frac{\partial q}{\partial t} = -\frac{v}{a}\frac{\partial q}{\partial \lambda} - \dot{\sigma}\frac{\partial q}{\partial \sigma} + \frac{g}{\Pi}\frac{\partial \tau_q}{\partial \sigma} + \frac{K_H}{a^2\cos\lambda}\frac{\partial}{\partial \lambda}\left(\cos\lambda\frac{\partial q}{\partial \lambda}\right) + S_L \quad (4.6)$$

$$\alpha = \frac{R\theta}{\sigma\Pi}\left(\frac{\sigma\Pi}{P_0}\right)^{\chi}. \quad (4.7)$$

Coordinates:

λ latitude
σ sigma

Model variables:

μ zonal wind speed
v meridional wind speed
Π surface pressure
Φ geopotential
θ potential temperature
q specific humidity
α specific volume

Forcing terms:

Q_R heating/cooling due to radiation
Q_L heating/cooling due to condensation processes
Q_S moisture source/sink due to condensation processes
$\tau_{u,v,\theta,q}$ vertical flux of momentum, heat and moisture,

where

$$\tau_x = \frac{g}{\alpha^2\Pi}K_\sigma\frac{\partial x}{\partial \sigma} \quad \text{for} \quad x = u, v, \theta, q$$

and

$$\tau_x = 0 \text{ at } \sigma = 0$$

$$\tau_{(u,v)} = -\frac{1}{\alpha}C_D|\vec{V}|(u, v)$$

$$\tau_\theta = \frac{1}{\alpha}C_D|\vec{V}|(\theta_s - \theta)$$

$$\tau_q = \frac{1}{\alpha}C_D|\vec{V}|(q_s - q)$$

at $\sigma = 1.0$; the subscript s denotes the surface and u, v, θ, and q are at the lowest model level.

Constants:

K_σ vertical diffusivity ($=0.2\ \text{m}^2\ \text{s}^{-1}$)
K_H horizontal diffusivity ($=5 \times 10^4\ \text{m}^2\ \text{s}^{-1}$)

C_D drag coefficients ($=1.5 \times 10^{-3}$)
a radius of the Earth
R gas constant of dry air
P_0 reference pressure ($=1000$ mb)

REFERENCES

Arakawa, A., and V. R. Lamb, 1977: Computational design of the basic dynamical processes of the UCLA general circulation model. *Methods in Computational Physics,* **17,** Academic Press, 174–265.

——, and M. J. Suarez, 1983: Vertical differencing of the primitive equations in sigma coordinates. *Mon. Wea. Rev.,* **111,** 34–45.

Bates, J. R., 1970: Dynamics of disturbances on the Intertropical Convergence Zone. *Quart. J. Roy. Meteor. Soc.,* **96,** 677–701.

Bjerknes, J., L. J. Allison, E. R. Kreins, F. A. Godshall, and G. Warnecke, 1969: Satellite mapping of the Pacific tropical cloudiness. *Bull. Amer. Meteor. Soc.,* **50,** 313–322.

Charney, J. G., 1971: Tropical cyclogenesis and the formation of the Intertropical Convergence Zone. *Mathematical Problems of Geophysical Fluid Dynamics,* W. H. Reid, Ed., *Lectures in Applied Mathematics,* Vol. 13, Amer. Math. Soc., 355–368.

——, 1974: Reply. *J. Atmos. Sci.,* **31,** 834–835.

——, and A. Eliassen, 1964: On the growth of hurricane depressions. *J. Atmos. Sci.,* **21,** 68–75.

——, E. Kalnay, E. K. Schneider, and J. Shukla, 1988: A study of the dynamics of the ITCZ in a symmetric atmosphere–ocean model. NASA Tech. Memo. 86220, 20 pp.

Davey, M. K., and A. E. Gill, 1987: Experiments on tropical circulation with a simple moist model. *Quart. J. Roy. Meteor. Soc.,* **113,** 1237–1269.

Emanuel, K., 1991: A scheme for representing cumulus convection in large-scale models. *J. Atmos. Sci.,* **48,** 2313–2335.

Garcia, O., 1985: Atlas of highly reflective clouds for the global tropics: 1971–1983. U.S. Dept. of Commerce, NOAA/Environmental Research Lab., Boulder, CO.

Gill, A. E., 1980: Some simple solutions for heat-induced tropical circulation. *Quart. J. Roy. Meteor. Soc.,* **106,** 447–462.

——, 1982: *Atmosphere–Ocean Dynamics.* Int. Geophys. Ser., Vol. 30. Academic Press, 662 pp.

Goswami, B. N., J. Shukla, E. K. Schneider, and Y. C. Sud, 1983: Study of the dynamics of the intertropical convergence zone with a symmetric version of the GLAS Climate Model. *J. Atmos. Sci.,* **41,** 5–19.

Graham, N. E., and T. P. Barnett, 1987: Sea surface temperature, surface wind divergence, and convection over tropical oceans. *Science,* **238,** 657–659.

Hack, J. J., W. H. Shubert, D. E. Stevens, and H. C. Kuo, 1989: Response of the Hadley circulation to convective forcing in the ITCZ. *J. Atmos. Sci.,* **46,** 2957–2973.

Hayashi, Y. Y., and A. Sumi, 1986: The 30–40 day oscillations simulated in an "aqua-planet" model. *J. Meteor. Soc. Japan,* **64,** 451–467.

Held, I. M., and A. Y. Hou, 1980: Nonlinear axially symmetric circulations in a nearly inviscid atmosphere. *J. Atmos. Sci.,* **37,** 515–533.

Hess, P. G., D. S. Battisti, and P. J. Rasch, 1992: The maintenance of the intertropical convergence zones and the large-scale circulation on a water-covered earth. *J. Atmos. Sci.,* **50,** 691–713.

Hirst, A. C., 1986: Unstable and damped equatorial modes in simple coupled ocean–atmosphere models. *J. Atmos. Sci.,* **43,** 606–630.

Holton, J. R., 1974: Comments on "Movable CISK." *J. Atmos. Sci.,* **31,** 833–834.

——, J. M. Wallace, and J. A. Young, 1971: On boundary layer dynamics and the ITCZ. *J. Atmos. Sci.,* **28,** 275–180.

Hou, A. Y., and R. S. Lindzen, 1992: The influence of concentrated heating on the Hadley circulation. *J. Atmos. Sci.,* **49,** 1233–1241.

Kuo, H.-L., 1974: Further studies of the parameterization of the influence of cumulus convection on large-scale flow. *J. Atmos. Sci.,* **31,** 1232–1240.

Lindzen, R. S., 1974: Wave–CISK in the tropics. *J. Atmos. Sci.,* **31,** 156–179.

——, 1990: *Dynamics in Atmospheric Physics.* Cambridge University Press, 310 pp.

——, and S. Nigam, 1987: On the role of sea surface temperature gradients in forcing low-level winds and convergence in the tropics. *J. Atmos. Sci.,* **44,** 2418–2436.

——, and A. Y. Hou, 1988: Hadley circulation for zonally averaged heating centered off the equator. *J. Atmos. Sci.,* **45,** 2416–2427.

Lorenz, E. N., 1967: *The Nature and Theory of the General Circulation of the Atmosphere.* World Meteorological Organization Monogr. No. 218, TP 115, 161 pp.

MacCracken, M. C., and S. J. Ghan, 1988: Design and use of zonally-symmetric climate models. *Physically-Based Modelling and Simulations of Climate and Climate Change,* M. E. Schlesinger, Ed., Kluwer Academic, NATO ASI Ser., 755–809.

Manabe, S., and R. F. Strickler, 1964: Thermal equilibrium of the atmosphere with a convective adjustment. *J. Atmos. Sci.,* **21,** 361–385.

——, J. Smagorinsky, and R. F. Strickler, 1965: Simulated climatology of a general circulation model with a hydrologic cycle. *Mon. Wea. Rev.,* **93,** 769–798.

Matsuno, T., 1966: Quasi-geostrophic motions in the equatorial area. *J. Meteor. Soc. Japan,* **44,** (No. 1), 25–43.

Morcrette, J.-J., 1991: Radiation and cloud radiative properties in the European Centre for Medium Range Weather Forecasts forecasting system. *J. Geophys. Res.,* **96** (D5), 9121–9132.

Neelin, J. D., 1988: A simple model for surface stress and low level flow in the tropical atmosphere driven by prescribed heating. *Quart. J. Roy. Meteor. Soc.,* **114,** 747–770.

——, 1989: On the interpretation of the Gill model. *J. Atmos. Sci.,* **46,** 2466–2468.

Oort, H., 1983: *Global Atmospheric Circulation Statistics, 1958–1973.* NOAA Prof. Paper No. 4. U.S. Govt. Printing Office, Washington, DC, 180 pp.

——, and E. M. Rasmusson, 1970: On the annual variation of the monthly mean meridional circulation. *Mon. Wea. Rev.,* **98,** 423–442.

Philander, S. G. H., T. Yamagata, and R. C. Pacanowski, 1984: Unstable air–sea interactions in the tropics. *J. Atmos. Sci.,* **41,** 604–613.

Pike, A. C., 1971: The inter-tropical convergence zone studied with an interacting atmosphere and ocean model. *Mon. Wea. Rev.,* **99,** 469–477.

Reed, R. J., and E. E. Recker, 1971: Structure and properties of synoptic-scale wave disturbances in the equatorial western Pacific. *J. Atmos. Sci.,* **28,** 1117–1133.

Reynolds, R. W., 1988: A real-time global sea surface temperature analysis. *J. Climate,* **1,** 75–86.

Salby, M. L., H. H. Hendon, K. Woodberry, and K. Tanaka, 1991: Analysis of global cloud imagery from multiple satellites. *Bull. Amer. Meteor. Soc.,* **72,** 467–480.

Schneider, E. K., 1977: Axially symmetric steady state for instability and climate studies. Part II. Nonlinear calculations. *J. Atmos. Sci.,* **34,** 280–296.

8——, and R. S. Lindzen, 1977: Axially symmetric steady state for instability and climate studies. Part I. Linearized calculations. *J. Atmos. Sci.,* **34,** 263–279.

Sumi, A., 1992: Pattern formation of convective activity over the aqua-planet with globally uniform sea surface temperature (SST). *J. Meteor. Soc. Japan,* **70,** 855–876.

Waliser, D. E., 1992: The preferred latitudes of the intertropical convergence zone: Observations and theory. Ph.D. dissertation,

Scripps Institution of Oceanography, University of California, San Diego, CA, 170 pp.

——, and C. Gautier, 1993: A global climatology of the ITCZ. *J. Climate,* **6,** 2162–2174.

——, N. E. Graham, and C. Gautier, 1993: Comparison of the highly reflective cloud and outgoing longwave datasets for use in estimating tropical deep convection. *J. Climate,* **6,** 331–353.

Williamson, D. L., J. T. Kiehl, V. Ramanathan, R. E. Dickinson, and J. J. Hack, 1987: Description of NCAR Community Climate Model (CCM1). NCAR Tech. Note, NCAR, Boulder, CO, 112 pp.

Yanai, M., T. Maruyama, T. Nitta, and Y. Hayashi, 1968: Power spectra of large scale disturbances of the tropical Pacific. *J. Meteor. Soc. Japan,* **46,** 308–323.

Young, J. A., 1988: Boundary layer dynamics of tropical and monsoonal flows. *Monsoon Meterology,* C. P. Chang and T. N. Krishnamurti, Eds., Oxford Press, 461–500.

Zebiak, S. E., 1982: A simple atmospheric model of relevance to El Niño. *J. Atmos. Sci.,* **39,** 2017–2027.

——, 1986: Atmospheric convergence feedback in a simple model for El Niño. *Mon. Wea. Rev.,* **114,** 1263–1271.